MS-based proteomics and network analysis of Lipotoxicity caused by palmitic acid in normal human astrocytes and the response of tibolone treatment

Diego Julián Vesga-Jiménez[1], Cynthia Martín[1], Andrés Aristizabal[1], George E. Barreto[2,3]; Janneth González[1]

[1.] Department of Nutrition and Biochemistry, Faculty of Sciences, Pontificia Universidad Javeriana Bogotá, D.C., Colombia
[2.] Department of Biological Sciences, University of Limerick, Limerick, Ireland
[3.] Health Research Institute, University of Limerick, Limerick, Ireland

Abstract

Chronic exposure to high amounts of fatty acids such as palmitic acid has become risk factor for the development of different neurodegenerative diseases (NDs). In the brain, astrocytes play an important role in the metabolic inflammatory response as oxidative stress, endoplasmic reticulum stress, and autophagy impairment. Recent studies have shown that tibolone a synthetic steroid induces neuroprotective effects; but the molecular mechanisms upon exposure to pal remains largely unknown. Using a proteomic approach on normal human astrocytes subject to supraphysiological levels of palmitic acid as a model to induce cytotoxicity, we have identified more than 15 proteins linked to the lipotoxic effect of palmitic acid and more than 20 proteins that may be associated with the protective effects of tibolone against lipotoxicity. The pathways mainly involved in the lipotoxic damage are related to endoplasmic reticulum functions, protein translation and transport, autophagy, and the induction of proapoptotic signals. This work indicated that some of the effects generated by pal are regulated by tibolone administration. Suggesting that damage caused by palmitic acid in astrocytes involves different mechanisms at the same time and that the tibolone has the potential effect of ameliorating this damage.

Keywords: Mass Spectrometry., Human astrocytes; tibolone; palmitic acid; obesity; neuroprotection, proteomics, network analysis

Introduction

Obesity is defined as the excessive accumulation of fatty acids (FAs) in adipose tissue that could potentially be harmful to health (World Health Organization, 2016). The percentage of people with obesity in the world is growing, and this condition is an important risk factor for different chronic diseases that kill at least 2.8 million people each year (World Health Organization, 2020). Excess of fat in the diet leads to an increase in palmitic acid (pal) concentrations in the body (Carta et al., 2017; Tracey et al., 2018). Pal is the most common saturated fatty acid in the human body and is obtained either through diet or endogenously synthesized (Carta et al., 2017; Innis, 2016).

The metabolic alterations modify the functioning of the central nervous system (SNC) that is particularly sensitive to oxidative stress, due to high oxygen consumption and the enrichment of polyunsaturated fatty acids, making it very vulnerable to lipid peroxidation by changing the neuronal and glial environment (Tracey et al., 2018). Studies have shown that persons with obesity than have presented oxidative stress and injuries are prone to develop different NDs, including Alzheimer's (AD), Parkinson's (PD), and Huntington's Disease (Anderson et al., 2019; Cakir and Nillni, 2019; Korbecki and Bajdak-Rusinek, 2019; Shamim et al., 2018). Astrocytes are glial cells that supports the neuronal function, that are abnormally activated in central pathologies of the nervous system, where the prolonged consume of a high-fat diet (HFD) increase process like reactive astrogliosis, which represents a defense mechanism (Garzón et al., 2016; Liddelow and Sofroniew, 2019); thus, this type of glial cell is important for normal brain function due to its ability to promote neuroprotection (Acaz-Fonseca et al., 2014).

The exposure of astrocytes to high levels of pal can induce endoplasmic reticulum (ER) stress and impaired autophagy (Ortiz-Rodriguez et al., 2018), production of pro-inflammatory cytokines, oxidative stress, ceramide production, and astrocyte activation (Gupta et al., 2012; Liu et al., 2013a; Sofroniew, 2015). Furthermore, pal can activate toll-like receptors (TLRs) that lead to the activation of a signaling cascade mediated by the nuclear factor enhancing the kappa light chains of activated B cells (NF-κB) (Korbecki and Bajdak-Rusinek, 2019; Okun et al., 2009). Following nuclear activation and translocation, NF-κB can induce the production of inflammatory cytokines, such as tumor necrosis factor (TNF), interleukin (IL) -6, and IL-1 (Okun et al., 2009). The alteration of the homeostatic balance of pal in adipose and non-adipose tissues triggers lipotoxic damage (Sorensen et al., 2010; Unger et al., 2010). Different experimental findings identify these pro-inflammatory pathways and astrocytic mitochondrial dysfunction as the main contributors to different NDs (Liddelow and Sofroniew, 2019; van Horssen et al., 2019).

On the other hand, different studies have demonstrated the neuroprotective and neurotrophic actions of estrogens (as 17β-estradiol) along with its cognate receptors can influence in the function and structure of the SNC (Acaz-Fonseca et al., 2014; Liu et al., 2010). However, the potential health risks associated with exposure to estrogens, such as increased incidence of uterine and breast cancer, may prevent its long-term use (Arevalo et al., 2011; Karki et al., 2014b). Therefore, estrogen-like compounds have been used in studies as alternatives to obtain therapeutic agents as potential treatments for different NDs (Lopez-rodriguez et al., 2011; Lopez-Rodriguez et al., 2015). Among these, tibolone, a synthetic steroid, has attracted attention because it shows beneficial effects by reducing cell death and mitochondrial damage against pal (Ávila Rodriguez et al., 2014; De Aguilar and González De Aguilar, 2019; Del Río et al., 2020; Garzón et al., 2016; González-Giraldo et al., 2018; Kloosterboer, 2004; Lopez-Rodriguez et al., 2015; Martin-Jiménez et al., 2020). However, the mechanisms of action underlying its protective effects are largely unknown and need to be studied to have a better understanding of them.

Much has been learned about proteomics in NDs (Dozio and Sanchez, 2018; Rocchio et al., 2019); however, the complete set of proteins involved in lipotoxicity caused by palmitic acid in human astrocytes and the response of tibolone treatment has to be identified. To address this research gap, we performed MS-based proteomics and network analysis of human astrocyte cultures exposed to toxic concentrations of pal and the response of tibolone treatment. We overlaid these changes on a protein co-expression network analysis to ascertain how differentially expressed proteins could be driving the observed changes. We also investigated whether pre-treatment with tibolone could attenuate these observed changes induced by pal, finding the main changes induced by pal are related to translation and transport of proteins, autophagy, and apoptosis. Also, tibolone, returned the expression of some of those proteins to the levels similar to the vehicle and augmented proteins related to cell survival processes.

Methods

Cell culture

The Normal Human Astrocyte (NHA, Lonza CC-2565) was used for this study due to its inherent similarity to primary astrocytes in terms of morphology and function. NHA cells do express GFAP (Glial Fibrillary Acid Protein), a key marker of astrocytes. Three different batches of NHA cells (#0000612736, #00005656712, #0000514417) were cultivated in ABM medium (Lonza)

supplemented with SingleQuots supplements (Lonza), the 3 different batches were trypsinized in passage 2 and placed in flasks of 25cm2 at a density of 10.000 cells/cm2, the cells were incubated at 37ºC and 5% of CO2 by 12 days, ABM (Astrocytes basal medium) medium was changed every 2 days, as recommended by Lonza, until the cells reached a confluence near of an 80%, and then the different treatments were applied getting a total of 3 biological replicates and 2 technical replicates for each treatment.

Tibolone pre-treatment

Cells were treated with tibolone before the addition of pal. Tibolone (Lot T0827, Sigma, St Louis, MO, USA) was dissolved in 100% DMSO as a stock solution at 40 mM, and further dilutions were made with serum-free DMEM up to a final concentration of 0,000025%. The aliquots were stored at -20°C and each aliquot was used 3 times or less. Varying times and concentrations of tibolone treatment were tested, and 10 nM of tibolone for 24 h was found to best preserve cell viability upon palmitic acid treatment (Martin-Jiménez et al., 2020).

Palmitic acid treatment

NHA cells were washed with PBS1x and then treated with serum-free DMEM containing pal (Sigma), BSA (fatty acid-free bovine serum albumin; Sigma A2153) as a carrier protein, and carnitine (Sigma, St Louis, MO, USA) to transport the fatty acids into the mitochondrial matrix. Cells were treated at different times using distinct concentrations of pal. Previous results from Martin- Jiménez (et al., 2020) indicated that the optimal pal concentration was 2mM diluted in BSA 1.35% for 24h. The control group included 1.35% of BSA and 2mM carnitine (Martin-Jiménez et al., 2020).

Protein extraction and quantification

The protocol defined for protein extraction used the following preparation for 1 ml of lysis buffer composed of 720 ml RIPA buffer, Lonza;10 ml Sodium fluoride 10mM; 10 ml of proteases inhibitors Halt cocktail Thermo; 250 ml pyrophosphate 2,5mM; 10 ml orthovanadate 1mM. The media was removed, and the flask was washed with 1ml of cold 1X PBS and then we removed the PBS with a pipette. We added 72ml for a 25cm2 flask of the RIPA cocktail + protease inhibitors and was left for 10 minutes in the freezer at -4°C, then the entire surface was scraped and collected in an Eppendorf. At this point, the Eppendorf tubes were placed in ice for 30 min and vortexed for 10 to 15 seconds every 10 min. After the 30 mins we centrifugate at 15200 rpm and -4 °C for 13 min, and the supernatant was transferred to a new tube and frozen at -80 °C. The amount of protein per sample

was quantified by the Bicinchoninic acid assay (BCA) method with the Pierce ™ BCA Protein Assay Kit from Thermo Fisher scientific, following the instructions of the supplier.

Protein digestion and load in the Q- exactive

The protein pellet was then solubilized in 200µL of 6M urea and submitted to the UC Davis Proteomics Core. For digestion 200mM of dithiothreitol (DTT) was added to a final concentration of 5mM and samples were incubated for 30min at 37°C. Next, 20mM iodoacetamide (IAA) was added to a final concentration of 15mM and incubated for 30min at room temp, followed by the addition of 20 µL DTT to quench the IAA. Lys-c was added to the sample and incubated for 2 hours at 30°C. Samples were then diluted to >1M urea by the addition of 50mM AMBIC and trypsin was added, and the samples were digested overnight at 37°C. The following day, samples were desalted using the Macro Spin Column (Nest Group).

Digested peptides were analyzed by LC-MS/MS on a Thermo Scientific Q-Exactive Orbitrap Mass spectrometer in conjunction with Proxeon Easy-nLC II HPLC (Thermo Scientific) and Proxeon nanospray source. The digested peptides were loaded a 100-micron x 25 mm Magic C18 100Å 5U reverse-phase trap where they were desalted online before being separated using a 75-micron x 150 mm Magic C18 200Å 3U reverse-phase column. Peptides were eluted using a 180-minute gradient with a flow rate of 300nl/min. An MS survey scan was obtained for the m/z range 300-1600, MS/MS spectra were acquired using a top 15 method, where the top 15 ions in the MS spectra were subjected to HCD (High Energy Collisional Dissociation). An isolation mass window of 2.0 m/z was for the precursor ion selection, and normalized collision energy of 27% was used for fragmentation. A twenty-second duration was used for dynamic exclusion.

Raw files processing for protein identification

The files were processed using the following parameters, a maximum miss cleavage of 2, in ion precursor identification a minimum of 50%, the search of razor and unique peptides, we obtained the validated proteins from SwissProt human as the database. The label-free-quantification was generated with proteome discoverer 2.3 using the search engine Sequest and AMANDA. Also, the results were processed using MaxQuant v1.6.10.43 and Perseus v 1.6.10.45 to compare the number of valid proteins and identified peptides. determining that the results with more proteins and better clustering of the samples were results obtained with Sequest.

Normalization and statistics for relative quantification

Protein intensities (Non-normalized) were imported into the R statistical programming software environment version 4.0.1 (R Core Team, 2019) for processing and statistical analysis of data. Data were transformed with (log2) almost routinely made to obtain a more symmetrical distribution before statistical analysis and all proteins with 70% valid values per group (comprising 6 replicates in each group) were kept (Karpievitch et al., 2012).

Normalization was performed by the Variance Stabilization Normalization (VSN) method, one of the non-linear methods that aim to maintain constant variance throughout the range of data and approaches the logarithm of large values to eliminate heteroscedasticity using the inverse hyperbolic sine (Huber et al., 2002).

The imputation of missing values was performed by K-nearest Neighbor Imputation (KNN) aims to identify k features that are very similar to the proteins with missing values, where the similarity is estimated by the Euclidean distance measure, and the missing values are imputed with the values of the weighted average from these neighboring proteins (Chai et al., 2014; Välikangas et al., 2017). Using a KNN value of 10 as suggested by Välikangas et al., (2017).

Differential expression analysis

The differential expression analysis was performed using the Optimized Reproducibility Test (ROTS) statistic, which classifies features according to their expression. The ROTS is a modified T-test aims to eliminate the bias in the data (Elo et al., 2008; Suomi et al., 2017). Differential expression was assessed between two pairs of conditions: 1) pal versus control (veh), pal with tibolone pre-treatment (condition tip) versus veh, and tip versus pal. Subsequently, the Q-value was calculated with the methods of pFDR, Benjamini Hochberg using the R package qvalue 2.18.0 Bioconductor https://www.bioconductor.org/packages/release/bioc/html/qvalue.html Storey JD, Bass AJ, Dabney A, Robinson D (2019). *qvalue: Q-value estimation for false discovery rate control*. R package version 2.18.0, http://github.com/jdstorey/qvalue. And with a Fold change (FC) ≥ ± 1.5 that is equivalent to a Log2 FC (LFC) ≥ ± 0.58.

Functional enrichment analysis

Following the recommendations made by Reimand (et al., 2019) Protein set enrichment analysis was conducted using g:Profiler online tool (Reimand et al., 2019) to search for the TOP 20 terms filtered by p-adjusted significance was set at Bonferroni-corrected threshold of $p < 0.05$ of the protein relationship across Gene Ontology terms giving priority to biological process and molecular function, pathways from KEGG, Reactome (Raudvere et al., 2019), and Human Protein Atlas HPA.

Protein co-expression network analysis

To determine the proteins with more interactions in the data set, we built a co-expression network analysis was done using the weighted correlation network analysis package (WGCNA) (https://horvath.genetics.ucla.edu/html/CoexpressionNetwork/Rpackages/WGCNA/, V1.68), employing the normalized protein abundances of all samples, with a soft threshold of 9 ($\beta=9$), and minimum module size of 20. Pearson correlation was used on the normalized protein abundances. Then, overlap for each module with the treatment, and all pal and tip differentially expressed proteins was assessed using Bonferroni-corrected Fisher's exact test p-values. Following this, the construction of PPI networks and identification of critical targets or hub proteins was built using the MCODE plugin of Cytoscape 3.8.0, the PPI network generated 4 clusters, and reduced from 355 nodes and 2657 edges to 110 nodes and 856 edges.

Finally, we intersected those hub proteins with the proteins differentially expressed with a q_value <0.05 in each comparison to determine proteins with high relevance in the network that were changing its expression with high confidence.

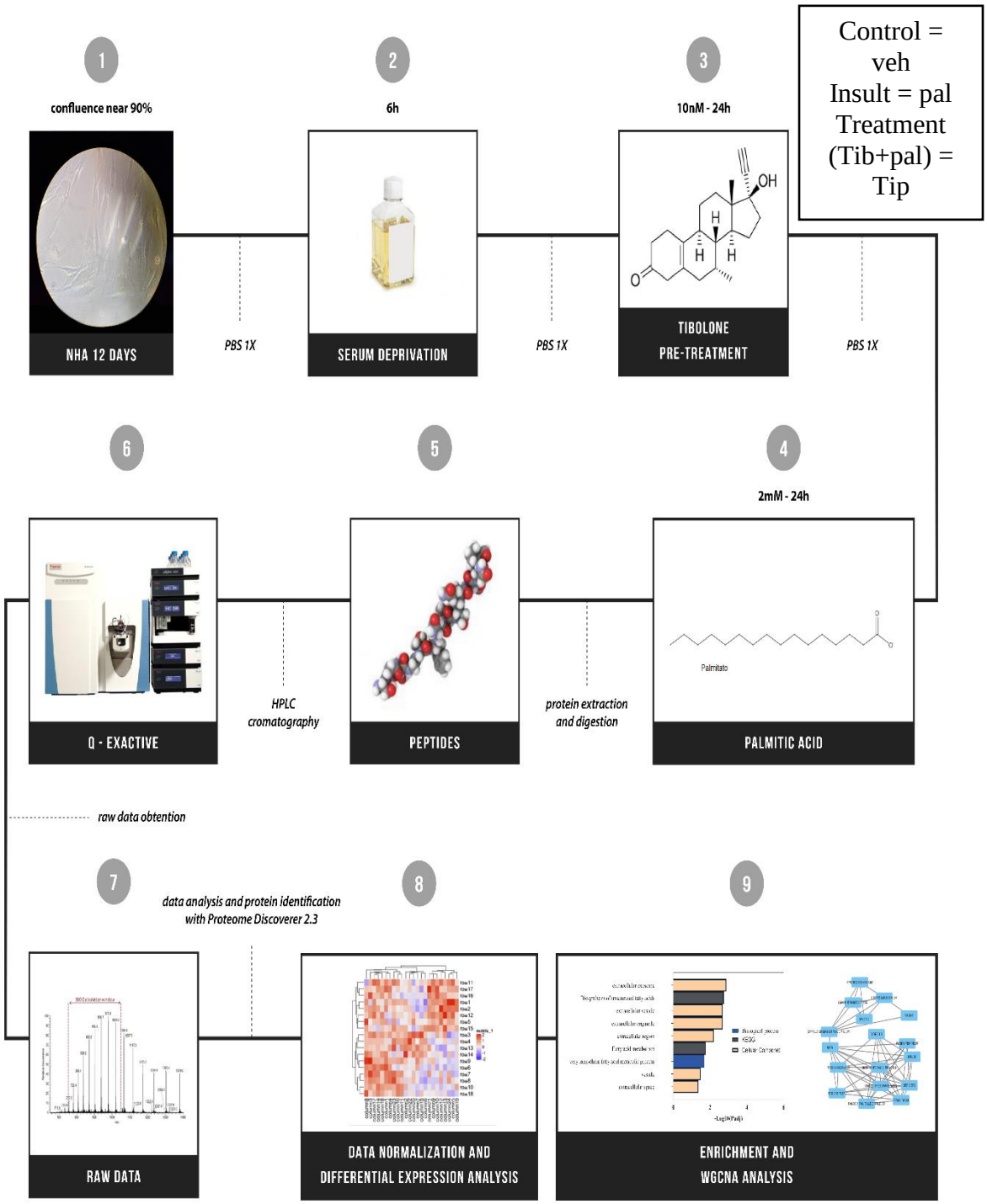

Fig 1. Graphic summary of the methodology

Results

Proteomic-wide profiling of palmitic acid-exposed astrocytes

Protein identification and relative quantification

To investigate the proteome alterations associated with pal-induced lipotoxicity in astrocytes, the procedures outlined in (Fig. 1) were followed, analyzing samples from 3 different biological replicates of the NHA cell line, called NHA1, NHA2, and NHA3, with 3 different conditions veh as control, pal as damage and tib_pal as a treatment to reduce pal damage, additionally a technical replica was made for each sample, for a total of 18 samples.

A global differential expression profile was made of the cultured astrocytes after pal treatment. Identifying 10,718 different peptide groups, corresponding to 1655 proteins identified with high confidence (FDR <0.01). Due to the stochastic nature of "shotgun" label-free or label-free quantitative proteomics, protein identification or abundance data may be missing in certain samples (Karpievitch et al., 2012). Proteins with missing data in any sample after using KNN were excluded from this analysis, resulting in the final quantification of 1281 proteins with complete data in all 18 samples.

The abundance of proteins acts as quality control, ensuring the amount of protein in each sample. After normalization, it was observed that the abundance of proteins was similar between the different conditions and samples used in the analysis (Fig. 2a). The heat map illustrated a general reproducibility, as well as the individual heterogeneity of the protein expression profiles, grouping the closest samples mainly by the treatment used in them and the second by the biological replicas and the treatment used in them (Fig. 2b).

Lists of proteins that were up-regulated and down-regulated in each comparison were generated (Supplementary Material 1, 2, 3). Between pal vs veh and tip vs veh, 31 shared proteins were found, all with the same expression pattern except for Q9UHB9 or the "SRP68 signal recognition particle subunit" that changed from a down-regulation in the pal vs comparison veh to regulation at high in tip vs veh (Fig. 5). On the other hand, pal vs veh compared with tip vs veh, showed 13 unique proteins up-regulated and 10 down-regulated, suggesting that tibolone returned those 23 proteins to expression levels as the control condition (Fig. 5) and these proteins are reported in (Table 5) and in their entirety in (supplementary material 4).

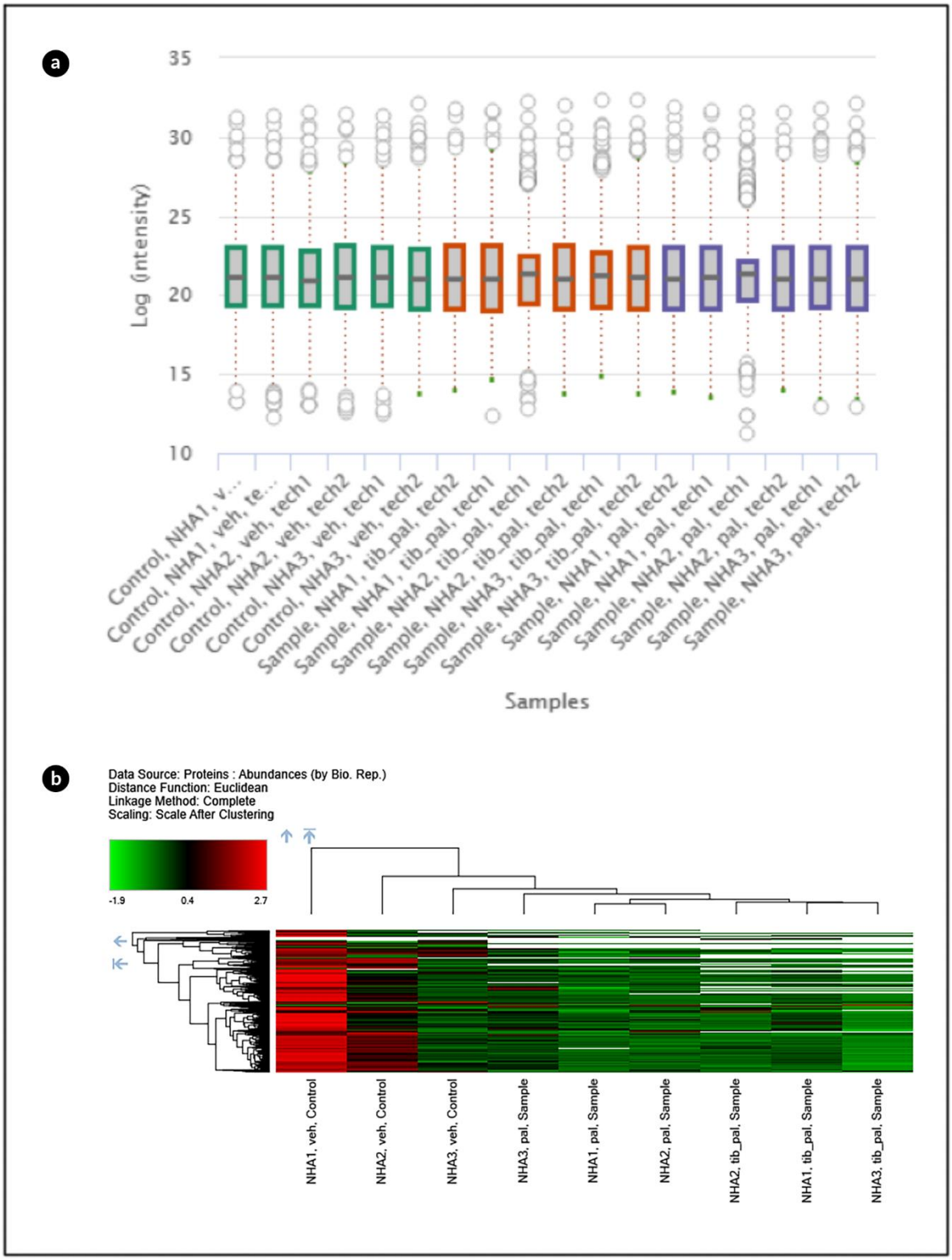

Fig 2. A Protein abundance for sample normalized with VSN method; B. HealthMap of protein abundance grouped for biological replicate and treatment, showing in red higher relative abundances and in green lower relative abundances

Functional enrichment analysis

To better understand the processes affected by the treatment with pal and tibolone, a functional enrichment analysis was performed to group the proteins in terms, to evaluate in a broader picture the changes in the cells using the terms more significant in g: profiler that exceeds the adjusted value threshold p <0.05. Comparing pal vs veh (Fig. 3), down-regulated proteins are enriched for the following terms, intracellular transport p_adj = 0.000116111, establishment of localization in the cell, cell localization, initiation of translation p_adj = 0.018303503, transport, processing of proteins in ER p_adj = 0.022648266, COPI-mediated transport, cellular response to stress, cellular response to external stimuli, retrograde Golgi transport to ER p_adj = 0.041526799. Meanwhile, the up-regulated proteins enriched for the following terms, in GO CC mainly to the extracellular space and the GO BP term of the metabolic process of very long chain FAs, and in terms of KEGG, FAs metabolism p_adj = 0.017043077 and biosynthesis of unsaturated FAs p_adj = 0.001779691. The results suggest that pal is downregulating the transport of proteins in the cell to different regions, particularly involvement in ER. Pal is also reducing translation initiation and is increasing processes related to the biosynthesis of FAs and their transformation to more complex molecules. Among the proteins that it regulates are the 3-ketoacyl-CoA peroxisomal thiolase EC 2.3.1.16 (ACAA1); Very long-chain enoyl-CoA reductase (TECR) and very-long-chain FAs elongation protein 1 (ELOVL1), which enrich the metabolism of very long chain FAs p_adj = 0.020697536 and for the metabolism of FAs p_adj = 0.017043077. Additionally, when observing the shared proteins between the tip_vs_pal and pal_vs_veh comparisons (Fig. 5 and Table 4), it is found that the down-regulated proteins enrich the synthesis of unsaturated FAs such as alpha-linoleic acid, suggesting that their synthesis is reducing. This is relevant because unsaturated FAs have protective effects in the brain, reducing inflammation and increasing their survival against lipotoxic damage by pal (Bazinet and Layé, 2014; Bentsen, 2017; Tracey et al., 2018).

In the comparison of tip vs veh (Fig. 4), the down-regulated proteins were enriched for terms related to transport and cell localization also reduced the response of infectious diseases and viral diseases, and the catabolic process of mRNA: p_adj = 0.004026028, GTP hydrolysis of 60S ribosomal unit p_adj = 0.009912779, the catabolic process of cellular macromolecules p_adj = 0.000940694. However, tibolone also increased proteins related to protein and cellular localization p_adj = 5.26E-05 and 5.06E-06 respectively, peptide transport p_adj = 0.000445928 and the immune effector process p_adj = 0.010693768. Therefore, at the enrichment level, it suggests that the protective effect of tibolone is probably related to the negative regulation of processes that affect protein synthesis and

counteract the dysregulation caused in transport and the localization of proteins, in addition to regulating proteins that are associated with the immune response.

The terms that were enriched for tip vs pal (Fig. 6) down-regulated proteins are extracellular organelles p_adj = 0.029179155, extracellular vesicle, extracellular exosome, cadherin binding p_adj = 0.042474795, cerebral cortex and endothelial cells p_adj = 0.026699216 and the terms for positively regulated proteins that are related to the COPII components vesicle layer p_adj = 0.010432134, ER exit site p_adj = 0.045836963 and surprisingly with thyroid cancer p_adj = 0.029670923. This suggests that the main differences between tip to pal are related to transport and vesicles, however, the number of proteins that showed differential expression in this comparison is small, and this could explain the enrichment of unexpected terms such as thyroid cancer, making necessary to inspect the role that proteins play individually, one by one, and not rely solely on enrichment analysis.

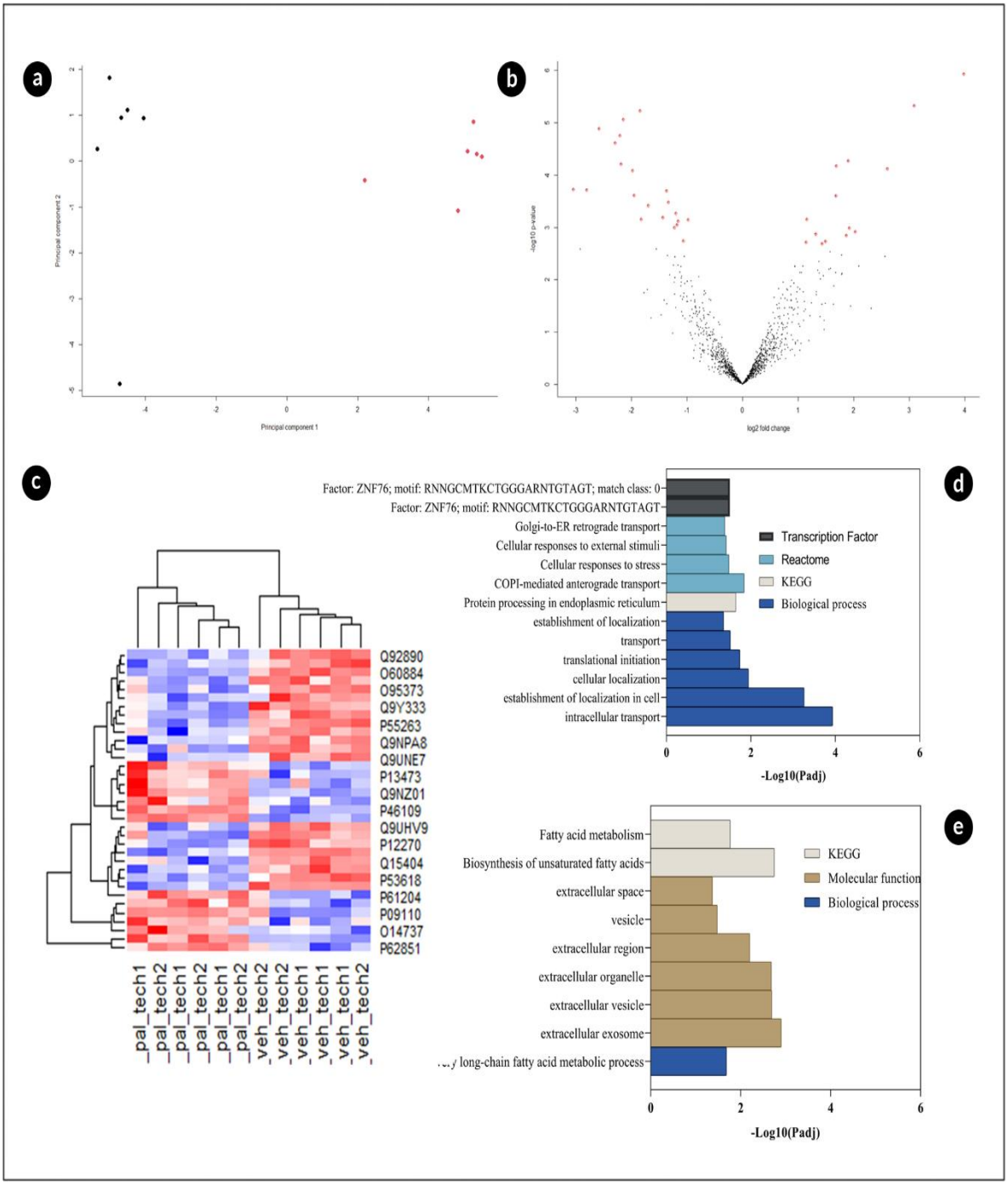

Fig 3. Differential expression of pal vs veh. a) PCA of the samples of pal in black and veh in red; b) heath map of proteins differentially expressed proteins with an FDR <0.05 in pal vs veh; c) Volcano plot showing differentially expressed proteins with a p-adjusted value of < 0.05; d) Enrichment analysis of up-regulated proteins in pal vs veh; e) Enrichment analysis of down-regulated proteins

Pal reduces proteins related to transcription and translation processes

Few studies have focused on the induction of changes produced by pal in the process of protein translation, and their effects on cells. At the nervous system level, none have been found to date, but

one of the effects of pal in the translation of pal in macrophages has been found, suggesting that pal reduces the translation process (Korbecki and Bajdak-Rusinek, 2019). Similarly, the results of the present study indicate that pal induces the expression of the eukaryotic initiation factor 2α (eIF2α), which induces the repression of translation (He et al., 2018; Korbecki and Bajdak-Rusinek, 2019); Besides, the results (Table 1) showed that pal negatively regulated the expression of subunit 1 of eukaryotic translation initiation factor 2 (eIF2S1) p = 0.00418306 and LFC = -1.14091479, this protein acts in the first steps of protein synthesis, forming a ternary complex with GTP and as an initiator of RNA translation (Mikami et al., 2006), however, it also has the dual ability to repress protein translation (Korbecki and Bajdak-Rusinek, 2019). Nevertheless, phosphorylation of eIF2α does not necessarily lead to down-regulation of global translation (Boye and Grallert, 2020).

Among other processes evidenced, it was found that pal down-regulated different proteins related to translation, such as the ribosomal protein 60S L37 (RPL37) p = 0.00024395 and LFC = -1.955268045, a protein that belongs to a segment of the 60S ribosomal subunit and protein translation. Also, pal negatively regulated Importin-7 (IPO7) p = 0.000647151 and LFC = -1.4343906, a protein responsible for transporting the protein to the nucleus (Gaudet et al., 2011), such as the ribosomal proteins RPL23A, RPS7, and RPL5 (Jäkel and Görlich, 1998), histones H2A, H2B, H3 and H4 (Jäkel et al., 1999). mRNA export and transcription factor (ENY2) p = 0.000382123 and LFC = -1.696939985, a protein involved in the activation of transcription-coupled to mRNA export (Zhao et al., 2008), eukaryotic translation initiation factor 4 gamma 2 (eIF4G2) p = 0.002612802 and LFC = -2.91627833, a protein related to the initiation of translation, in addition, Kar et. Al. (2013) reported that down-regulation of axonal expression of eIF4G2 also inhibited local protein synthesis and axon growth (Kar et al., 2013).

A reduction in transcription can result in a reduction in translation (Slobodin et al., 2017). The dysregulation of proteins related to transcription and translation suggests a mechanism, by which, exposure to pal can indirectly lead to ER stress, oxidative stress, and inflammatory responses due to the dysregulation of factors such as eIF4 and eIF2α and other proteins related to the translation initiation process such as RPL37 and IPO7 that regulate other RPLs (Korbecki and Bajdak-Rusinek, 2019; Liu and Qian, 2014). This could support the different stress pathways in the mechanism proposed by Korbecki et al., (2019) in macrophages treated by pal, suggesting that the reduction in translation related to eLF4 leads to ER stress, inflammation, and cell death (Korbecki and Bajdak-Rusinek, 2019).

Table 1 Differentially expressed proteins in the comparison of pal vs veh

Entry	Protein names	Gene names	Protein expression
P60484	Phosphatidylinositol 3,4,5-trisphosphate 3-phosphatase and dual-specificity protein phosphatase PTEN (EC 3.1.3.16) (EC 3.1.3.48) (EC 3.1.3.67) (Mutated in multiple advanced cancers 1) (Phosphatase and tensin homolog)	PTEN MMAC1 TEP1	Up-regulated
P13473	Lysosome-associated membrane glycoprotein 2 (LAMP-2) (Lysosome-associated membrane protein 2) (CD107 antigen-like family member B) (LGP-96) (CD antigen CD107b)	LAMP2	Up-regulated
O14737	Programmed cell death protein 5 (TF-1 cell apoptosis-related protein 19) (Protein TFAR19)	PDCD5 TFAR19	Up-regulated
Q9NZ01	Very-long-chain enoyl-CoA reductase (EC 1.3.1.93) (Synaptic glycoprotein SC2) (Trans-2,3-enoyl-CoA reductase) (TER)	TECR GPSN2 SC2	Up-regulated
Q9UJU6	Drebrin-like protein (Cervical SH3P7) (Cervical mucin-associated protein) (Drebrin-F) (HPK1-interacting protein of 55 kDa) (HIP-55) (SH3 domain-containing protein 7)	DBNL CMAP SH3P7 PP5423	Up-regulated
P09913	Interferon-induced protein with tetratricopeptide repeats 2 (IFIT-2) (ISG-54 K) (Interferon-induced 54 kDa protein) (IFI-54K) (P54)	IFIT2 CIG-42 G10P2 IFI54 ISG54	Up-regulated
P78344	Eukaryotic translation initiation factor 4 gamma 2 (eIF-4-gamma 2) (eIF-4G 2) (eIF4G 2) (Death-associated protein 5) (DAP-5) (p97)	EIF4G2 DAP5 OK/SW-cl.75	Down-regulated
P61927	60S ribosomal protein L37 (G1.16) (Large ribosomal subunit protein eL37)	RPL37	Down-regulated
O95373	Importin-7 (Imp7) (Ran-binding protein 7) (RanBP7)	IPO7 RANBP7	Down-regulated
Q92890	Ubiquitin recognition factor in ER-associated degradation protein 1 (Ubiquitin fusion degradation protein 1) (UB fusion protein 1)	UFD1 UFD1L	Down-regulated
Q9NPA8	Transcription and mRNA export factor ENY2 (Enhancer of yellow 2 transcription factor homolog)	ENY2 DC6	Down-regulated
P61313	60S ribosomal protein L15 (Large ribosomal subunit protein eL15)	RPL15 EC45 TCBAP0781	Down-regulated
P05198	Eukaryotic translation initiation factor 2 subunit 1 (Eukaryotic translation initiation factor 2 subunit alpha) (eIF-2-alpha) (eIF-2A) (eIF-2alpha)	EIF2S1 EIF2A	Down-regulated
Q9UNE7	E3 ubiquitin-protein ligase CHIP (EC 2.3.2.27) (Antigen NY-CO-7) (CLL-associated antigen KW-8) (Carboxy terminus of Hsp70-interacting protein) (RING-type E3 ubiquitin transferase CHIP) (STIP1 homology and U box-containing protein 1)	STUB1 CHIP PP1131	Down-regulated
Q92890	Ubiquitin recognition factor in ER-associated degradation protein 1 (Ubiquitin fusion degradation protein 1) (UB fusion protein 1)	UFD1 UFD1L	Down-regulated

List of proteins that were differentially expressed with a p_value < 0.01 and FDR< 0.1 in the comparison of pal vs veh.

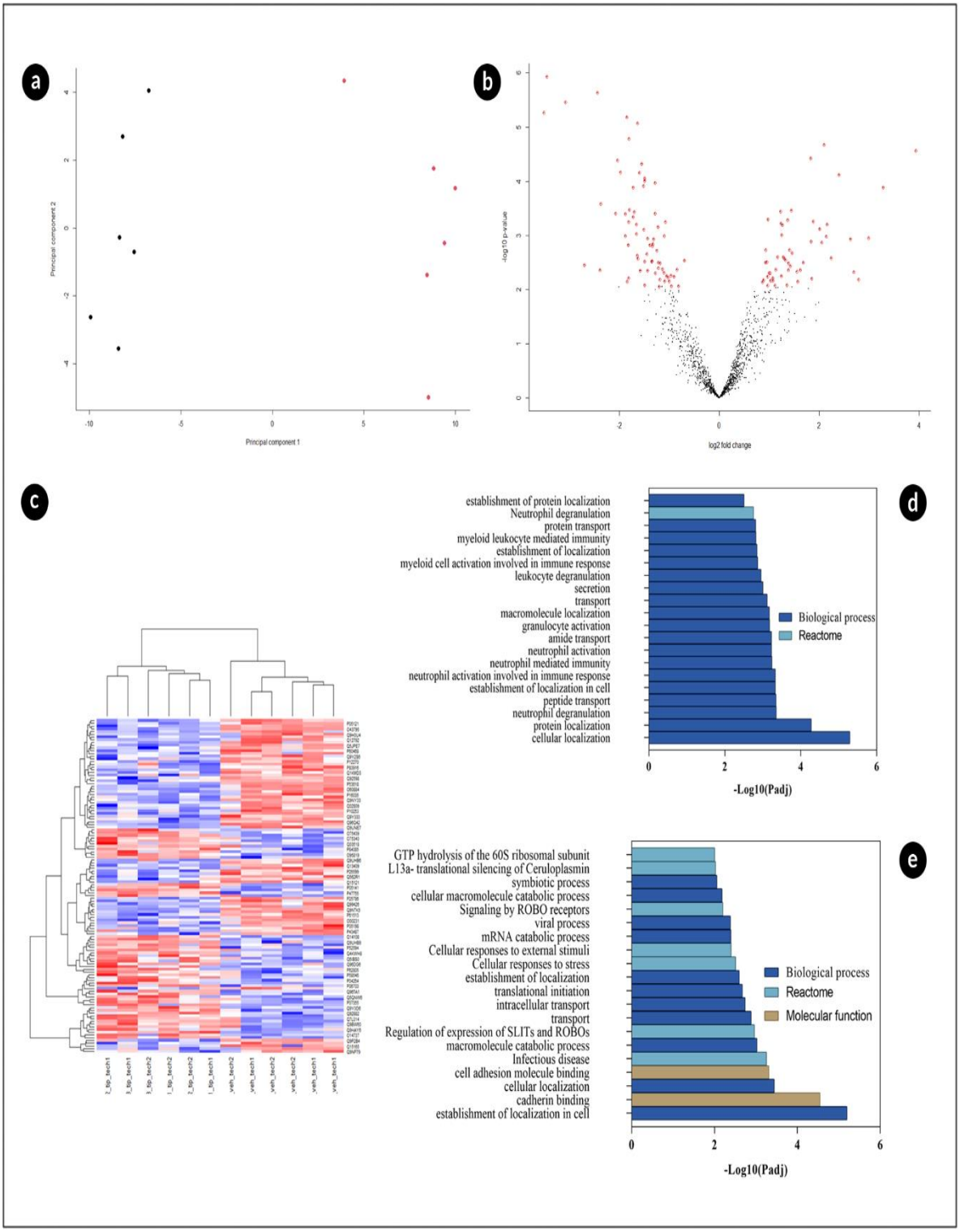

Fig 4. Differential expression of tip vs veh. a) PCA of the samples of pal in black and veh in red; b) heath map of proteins differentially expressed proteins with an FDR <0.05 in tip vs veh; c) Volcano plot showing differentially expressed proteins with a p-adjusted value of < 0.05; d) enrichment analysis of up-regulated proteins in tib vs veh; e) Enrichment analysis of down-regulated proteins

Palmitic acid affects autophagy and up-regulates proapoptotic pathways

It is known that pal induces cell death in astrocytes (González-Giraldo et al., 2018; Martin-Jiménez et al., 2020; Ng and Say, 2018), and it has been reported to be related to the reduction of the autophagy process (Ortiz-Rodriguez et al., 2018; Ortiz-Rodriguez and Arevalo, 2020). Therefore, the effects of pal on autophagy and activation of pro-apoptotic pathways in human astrocytes were investigated. Observing expression changes consistent with these effects (Table 1). Finding ubiquitin-protein ligase E3 strongly up-regulated by pal CHIP (STUB1) p = 0.000191257 and LFC = -2.805049685, this protein has a fundamental role in the protein folding process directed at misfolded chaperone substrates towards proteasomal degradation and it probably induces the poly ubiquitination that is necessary for protein degradation (Shang et al., 2014). Besides, pal down-regulated the expression of the ubiquitin recognition factor in the ER 1-associated degradation protein (UFD1) p = 0.000199063 and LFC = -1.369768858 which is a key component for the ubiquitin-dependent proteolytic pathway for the degradation of misfolded proteins (Gaudet et al., 2011). In addition, pal up-regulates proapoptotic proteins such as programmed cell death protein 5 (PDCD5) p = 0.001415301 and LFC = 1.864688494 and interferon-induced protein with tetratricopeptide repeats 2 (IFIT2) p = 0.003626464 and CFL = 2.561125172. Up-regulation of PDCD5 and IFIT2, combined with down-regulation of STUB1 and UFD1, suggest a mechanism by which exposure to palmitic acid may lead to a disruption of autophagy and the induction of apoptosis. Surprisingly, at the protein level, pal-induced damage in NHA cells was not strongly related to oxidative stress or inflammatory response. However, many pal proteins are related to the term neutrophil degranulation and this could indirectly indicate that pal is causing inflammation.

Tibolone returns different proteins to expression levels comparable to the vehicle

Differentially expressed proteins were compared in the comparison between pal and veh and the comparison of tip vs veh (Table 2), following the logic that the tip condition is tibolone with pal, all the unique proteins in pal should be present in tip unless tip modifies its expression. The results show that tibolone returned 23 proteins to expression levels similar to those of the vehicle (Table 2), among them RPL37, eIF4G2, IPO7, which, as mentioned previously, have an important role in the regulation of protein translation. Suggesting that the protective effect of tibolone on NHA cells is related to the transport processes of proteins mainly to the RE and by vesicles to different compartments; According to the results of GOSlim (Supplementary Material 5) it is observed that if the down-regulation of protein transport affects the transport of peptides, amines, macromolecules and the establishment of proteins in the compartments, therefore it would affect the functioning of the ER and the possible destinations of these vesicles; it is suggested that if tibolone reverts the expression of these proteins

411 to vehicle-like expression. It also returned to levels of expression similar to those of the control of the
412 proteins related to the translation process, which could preliminarily prevent the induction of different
413 processes such as inflammation, ER stress, or cell death (Korbecki and Bajdak-Rusinek, 2019).
414
415 Table 2 Differentially expressed proteins in the comparison of tip vs veh
416

Entry	Protein names	Gene names	Protein expression
O95819	Mitogen-activated protein kinase kinase kinase kinase 4 (EC 2.7.11.1) (HPK/GCK-like kinase HGK) (MAPK/ERK kinase kinase kinase 4) (MEK kinase kinase 4) (MEKKK 4) (Nck-interacting kinase)	MAP4K4 HGK KIAA0687 NIK	Up-regulated
Q9UHB9	Signal recognition particle subunit SRP68 (SRP68) (Signal recognition particle 68 kDa protein)	SRP68	Up-regulated
O75340	Programmed cell death protein 6 (Apoptosis-linked gene 2 protein homolog) (ALG-2)	PDCD6 ALG2	Up-regulated
P09914	Interferon-induced protein with tetratricopeptide repeats 1 (IFIT-1) (Interferon-induced 56 kDa protein) (IFI-56K) (P56)	IFIT1 G10P1 IFI56 IFNAI1 ISG56	Up-regulated

Q14108	Lysosome membrane protein 2 (85 kDa lysosomal membrane sialoglycoprotein) (LGP85) (CD36 antigen-like 2) (Lysosome membrane protein II) (LIMP II) (Scavenger receptor class B member 2) (CD antigen CD36)	SCARB2 CD36L2 LIMP2 LIMPII	Up-regulated
P62851	40S ribosomal protein S25 (Small ribosomal subunit protein eS25)	RPS25	Up-regulated
P60484	Phosphatidylinositol 3,4,5-trisphosphate 3-phosphatase and dual-specificity protein phosphatase PTEN (EC 3.1.3.16) (EC 3.1.3.48) (EC 3.1.3.67) (Mutated in multiple advanced cancers 1) (Phosphatase and tensin homolog)	PTEN MMAC1 TEP1	Up-regulated
P29692	Elongation factor 1-delta (EF-1-delta) (Antigen NY-CO-4)	EEF1D EF1D	Up-regulated
Q5QNW6	Histone H2B type 2-F (H2B-clustered histone 18)	H2BC18 HIST2H2BF	Up-regulated
O14879	Interferon-induced protein with tetratricopeptide repeats 3 (IFIT-3) (CIG49) (ISG-60) (Interferon-induced 60 kDa	IFIT3 CIG-49 IFI60 IFIT4 ISG60	Up-regulated

	protein) (IFI-60K) (Interferon-induced protein with tetratricopeptide repeats 4) (IFIT-4) (Retinoic acid-induced gene G protein) (P60) (RIG-G)		
P62805	Histone H4	H4C1 H4/A H4FA HIST1H4A; H4C2 H4/I H4FI HIST1H4B; H4C3 H4/G H4FG HIST1H4C; H4C4 H4/B H4FB HIST1H4D; H4C5 H4/J H4FJ HIST1H4E; H4C6 H4/C H4FC HIST1H4F; H4C8 H4/H H4FH HIST1H4H; H4C9 H4/M H4FM HIST1H4I; H4C11 H4/E H4FE HIST1H4J; H4C12 H4/D H4FD HIST1H4K; H4C13 H4/K H4FK HIST1H4L; H4C14 H4/N H4F2 H4FN HIST2H4 HIST2H4A; H4C15 H4/O H4FO HIST2H4B; H4-16 HIST4H4	Up-regulated
P09913	Interferon-induced protein with tetratricopeptide repeats 2 (IFIT-2) (ISG-54 K) (Interferon-induced 54 kDa protein) (IFI-54K) (P54)	IFIT2 CIG-42 G10P2 IFI54 ISG54	Up-regulated
P53618	Coatomer subunit beta (Beta-coat protein) (Beta-COP)	COPB1 COPB MSTP026	Down-regulated
O43294	Transforming growth factor beta-1-induced transcript 1 protein (Androgen receptor	TGFB1I1 ARA55	Down-regulated

	coactivator 55 kDa protein) (Androgen receptor-associated protein of 55 kDa) (Hydrogen peroxide-inducible clone 5 protein) (Hic-5)		
Q9NX63	MICOS complex subunit MIC19 (Coiled-coil-helix-coiled-coil-helix domain-containing protein 3)	CHCHD3 MIC19 MINOS3	Down-regulated
Q04637	Eukaryotic translation initiation factor 4 gamma 1 (eIF-4-gamma 1) (eIF-4G 1) (eIF-4G1) (p220)	EIF4G1 EIF4F EIF4G EIF4GI	Down-regulated
P53618	Coatomer subunit beta (Beta-coat protein) (Beta-COP)	COPB1 COPB MSTP026	Down-regulated
O43294	Transforming growth factor beta-1-induced transcript 1 protein (Androgen receptor coactivator 55 kDa protein) (Androgen receptor-associated protein of 55 kDa) (Hydrogen peroxide-inducible clone 5 protein) (Hic-5)	TGFB1I1 ARA55	Down-regulated
Q9NX63	MICOS complex subunit MIC19 (Coiled-coil-helix-coiled-coil-helix domain-containing protein 3)	CHCHD3 MIC19 MINOS3	Down-regulated

Q04637	Eukaryotic translation initiation factor 4 gamma 1 (eIF-4-gamma 1) (eIF-4G 1) (eIF-4G1) (p220)	EIF4G1 EIF4F EIF4G EIF4GI	Down-regulated
Q13510	Acid ceramidase (AC) (ACDase) (Acid CDase) (EC 3.5.1.23) (Acylsphingosine deacylase) (N-acylethanolamine hydrolase ASAH1) (EC 3.5.1.-) (N-acylsphingosine amidohydrolase) (Putative 32 kDa heart protein) (PHP32) [Cleaved into: Acid ceramidase subunit alpha; Acid ceramidase subunit beta]	ASAH1 ASAH HSD-33 HSD33	Down-regulated
O43615	Mitochondrial import inner membrane translocase subunit TIM44	TIMM44 MIMT44 TIM44	Down-regulated
Q15404	Ras suppressor protein 1 (RSP-1) (Rsu-1)	RSU1 RSP1	Down-regulated
P05198	Eukaryotic translation initiation factor 2 subunit 1 (Eukaryotic translation initiation factor 2 subunit alpha) (eIF-2-alpha) (eIF-2A) (eIF-2alpha)	EIF2S1 EIF2A	Down-regulated

Q15121	Astrocytic phosphoprotein PEA-15 (15 kDa phosphoprotein enriched in astrocytes) (Phosphoprotein enriched in diabetes) (PED)	PEA15	Down-regulated

List of proteins that were differentially expressed with a p_value <0.01 and FDR< 0.1 in the comparison of tip vs veh.

a

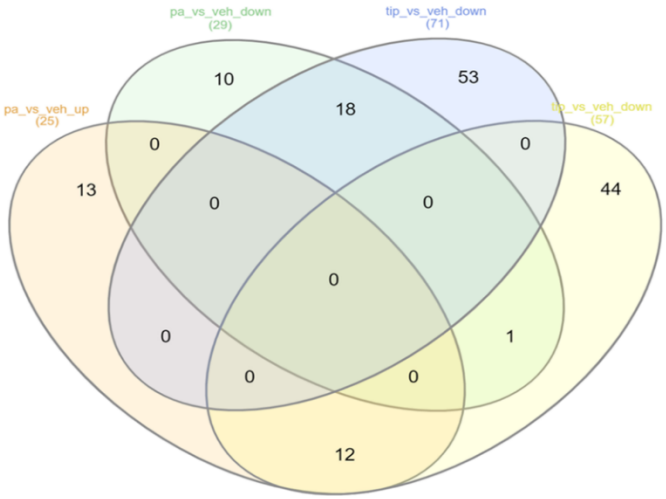

b

GO:BP		stats	
Term name	Term ID	p_{adj}	$-\log_{10}(p_{adj})$
alpha-linolenic acid metabolic process	GO:0036109	4.698×10^{-2}	

1 to 1 of 1 Page 1 of 1

KEGG		stats	
Term name	Term ID	p_{adj}	$-\log_{10}(p_{adj})$
Biosynthesis of unsaturated fatty acids	KEGG:01040	2.158×10^{-2}	

1 to 1 of 1 Page 1 of 1

REAC		stats	
Term name	Term ID	p_{adj}	$-\log_{10}(p_{adj})$
alpha-linolenic (omega3) and linoleic (omega6) acid metab...	REAC:R-HSA-20...	1.741×10^{-2}	
alpha-linolenic acid (ALA) metabolism	REAC:R-HSA-20...	1.741×10^{-2}	

1 to 2 of 2 Page 1 of 1

c

GO:MF		stats	
Term name	Term ID	p_{adj}	$-\log_{10}(p_{adj})$
cell adhesion molecule binding	GO:0050839	3.904×10^{-2}	

1 to 1 of 1 Page 1 of 1

GO:BP		stats	
Term name	Term ID	p_{adj}	$-\log_{10}(p_{adj})$
response to heat	GO:0009408	3.597×10^{-2}	

1 to 1 of 1 Page 1 of 1

KEGG		stats	
Term name	Term ID	p_{adj}	$-\log_{10}(p_{adj})$
Protein processing in endoplasmic reticulum	KEGG:04141	6.976×10^{-3}	

1 to 1 of 1 Page 1 of 1

FIG 5. a) Venn diagram of pal and tip vs veh, to difference the proteins up and downregulated in the different conditions compared with the vehicle. tip vs veh has 31 unique proteins that are up-regulated and 41 down-regulated; pal vs veh 9 proteins up-regulated and 24 down-regulated; between the corporations, there are 5 up-regulated y 8 down-regulated shared; b) functional enrichment of shared proteins that are down-regulated; c) functional enrichment of shared proteins that are up-regulated

Tibolone response against palmitic acid

The results show that tibolone increased the expression of some proteins enriched in terms of transporter proteins of vesicles such as COPII (Fig. 6 and Table 3), and reduced the expression of proteins with proapoptotic activity such as the Drebrin-like protein (DBNL) p = 2.77E-05 LFC = -3.104115258, additionally in comparison with veh IFIT3 up-regulated p = 0.001343872 and LFC = 2.054834577 and it is a protein that can reverse the effect of IFIT2 by negatively regulating apoptotic processes (Stawowczyk et al., 2011), while its expression remains unchanged in pal vs veh. It is important to note that tip augmented the expression of ribosomal proteins such as RPL23 p = 0.001775566 and LFC = 1.187426773 which is part of the 60s ribosomal subunit and is the largest subunit of the 80s ribosome that catalyzes the protein translation process (Odintsova et al., 2003), also, tip returned to the level of the vehicle the previously described protein eIF4G2 with p-value = 0.002254098 and LFC = 2.455214841. And increased the transport protein Sec24C (Sec24C) p = 0.002929742 LFC = 1.576720125 the programmed cell death protein 6 (PDCD6) p = 0.002007806 LFC = 1.339618944. The two proteins related to the formation of the COPII vesicle coating are also related to ER output, indicating that they are favoring cellular transport avoiding the dysregulation of protein localization. However, PDCD6 is considered a protein with pro-apoptotic activity, however, this protein can exert a negative regulation of cell proliferation (Chen et al., 2006) and this could be interesting to prevent gliosis damage since it is characterized by hypertrophy and uncontrolled proliferation of astrocytes (Pekny and Pekna, 2014).

tip reduced lysosomal alpha-glucosidase (GAA) with a p = 0.000159641 and an FDR = -1.701963592, which could suggest that tibolone is reducing glycogen catabolic processes (Roig-Zamboni et al., 2017) which are related to ROS production (Quijano et al., 2016). On the other hand, it was found that tip reduces the expression of cytoplasmic Aconitase (ACO1) with p = 1.41E-05 and FDR = -2.688103819, this protein is responsible for regulating iron homeostasis acting as a chelator (Lushchak et al., 2014) and this reduction could be harmful to cells. These results suggest that tibolone has some protective effects on NHA cells against the effects of pal. Its role was evidenced by

increasing the expression of transport proteins, favoring the correct localization of proteins. However, the role of some proteins is not entirely clear to which tibolone modulates the expression (Table 3 and supplementary material 3) and depending on the context could have detrimental effects.

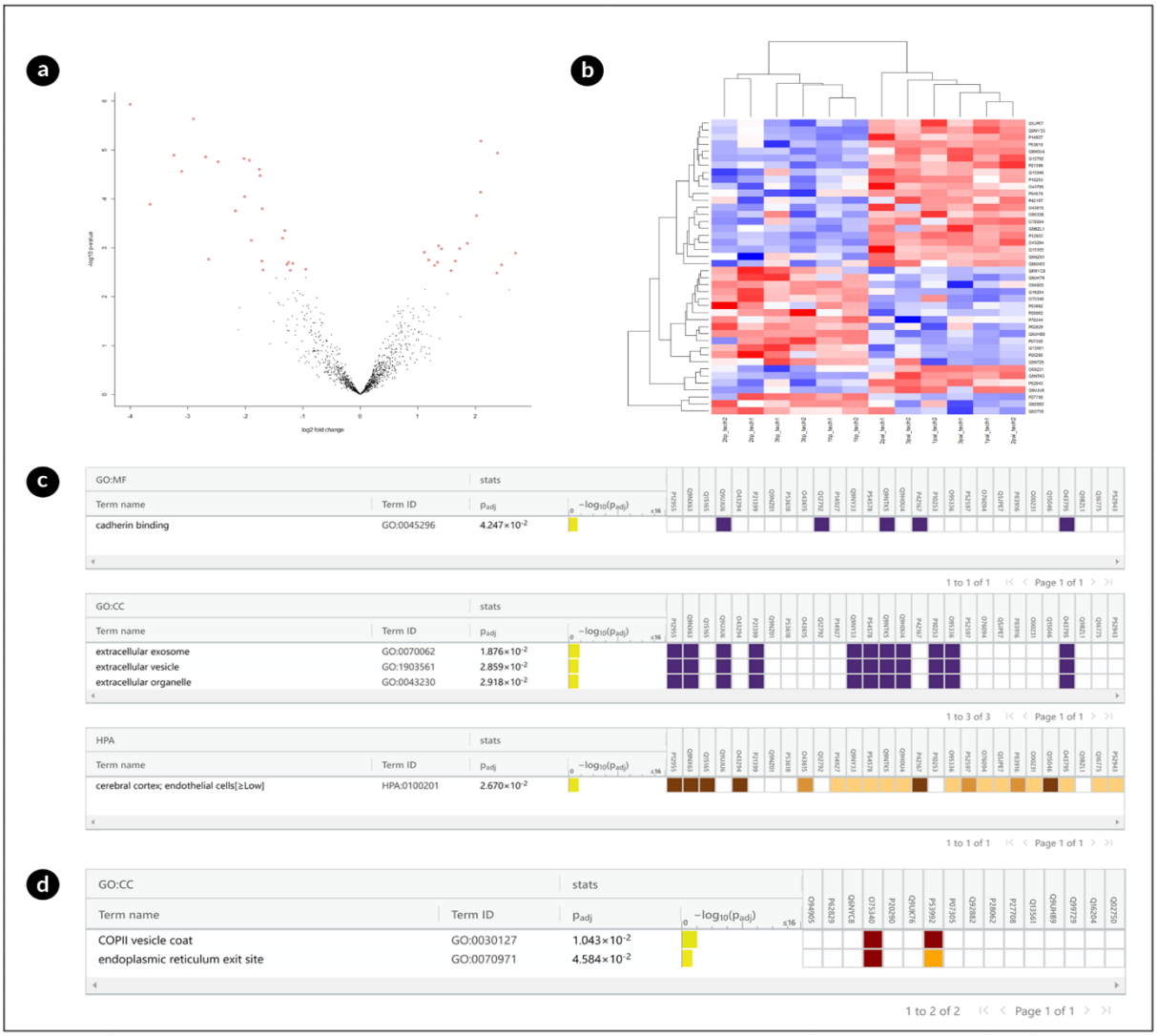

Fig 6. Differential expression of tip vs pal: a) normalized protein abundances of the samples treated with both condition; b) heath map of proteins differentially expressed proteins with a p- adjusted value <0.05 in pal vs veh; c) Volcano plot showing differentially expressed proteins with a p-adjusted value of < 0.05; d) enrichment analysis of down-regulated proteins in pal vs veh; e) Enrichment analysis of up-regulated proteins

Table 3 Differentially expressed proteins in the comparison of tip vs pal

Entry	Protein names	Gene names	Protein expression

P62829	60S ribosomal protein L23 (60S ribosomal protein L17) (Large ribosomal subunit protein uL14)	RPL23	Up-regulated
O75340	Programmed cell death protein 6 (Apoptosis-linked gene 2 protein homolog) (ALG-2)	PDCD6 ALG2	Up-regulated
Q13561	Dynactin subunit 2 (50 kDa dynein-associated polypeptide) (Dynactin complex 50 kDa subunit) (DCTN-50) (p50 dynamitin)	DCTN2 DCTN50	Up-regulated
Q9UHB9	Signal recognition particle subunit SRP68 (SRP68) (Signal recognition particle 68 kDa protein)	SRP68	Up-regulated
P78344	Eukaryotic translation initiation factor 4 gamma 2 (eIF-4-gamma 2) (eIF-4G 2) (eIF4G 2) (Death-associated protein 5) (DAP-5) (p97)	EIF4G2 DAP5 OK/SW-cl.75	Up-regulated
Q02750	Dual specificity mitogen-activated protein kinase kinase 1 (MAP kinase kinase 1) (MAPKK 1) (MKK1) (EC 2.7.12.2) (ERK activator kinase 1) (MAPK/ERK kinase 1) (MEK 1)	MAP2K1 MEK1 PRKMK1	Up-regulated
Q9NX63	MICOS complex subunit MIC19 (Coiled-coil-helix-coiled-coil-helix domain-containing protein 3)	CHCHD3 MIC19 MINOS3	Down-regulated
O43294	Transforming growth factor beta-1-induced transcript 1 protein (Androgen receptor coactivator 55 kDa protein) (Androgen receptor-associated protein of 55 kDa) (Hydrogen peroxide-inducible clone 5 protein) (Hic-5)	TGFB1I1 ARA55	Down-regulated
P21399	Cytoplasmic aconitate hydratase (Aconitase) (EC 4.2.1.3) (Citrate hydro-lyase) (Ferritin repressor protein) (Iron regulatory protein 1) (IRP1) (Iron-responsive element-binding protein 1) (IRE-BP 1)	ACO1 IREB1	Down-regulated
P54578	Ubiquitin carboxyl-terminal hydrolase 14 (EC 3.4.19.12) (Deubiquitinating enzyme 14) (Ubiquitin thioesterase 14) (Ubiquitin-specific-processing protease 14)	USP14 TGT	Down-regulated
P10253	Lysosomal alpha-glucosidase (EC 3.2.1.20) (Acid maltase) (Aglucosidase alfa) [Cleaved into: 76 kDa lysosomal alpha-glucosidase; 70 kDa lysosomal alpha-glucosidase]	GAA	Down-regulated
O76094	Signal recognition particle subunit SRP72 (SRP72) (Signal recognition particle 72 kDa protein)	SRP72	Down-regulated
O00231	26S proteasome non-ATPase regulatory subunit (11; RPN6; S9)	PSMD11	Down-regulated

List of proteins that were differentially expressed with a p_value < 0.01 and FDR< 0.1 in the comparison of tip vs pal.

Table 4 shared proteins of treatments compared with the control

Shared Down	Shared Up
Q96Q42	Q12904
Q9UNE7	P60484
P55263	P00403
P48047	Q9BW60
Q9Y333	Q9UBI6
Q9P2B4	P62851
Q15404	O14737
O60884	Q96DG6
P16035	Q92888
Q92890	P09913
P12270	P09110
O00571	P13010
O43795	
P61313	
Q14677	
P05198	
Q13409	
Q9UHB9	Q9UHB9(up_regulated in tip_vs_veh)
P53618	

Table 4. In this table we see the proteins that are shared between the comparison of pal vs veh and tip vs veh, seeing that almost all the proteins shared maintain a similar pattern of expression except Q9UHB9 that switches from down-regulated in pal vs veh to up-regulated in tip vs veh

Table 5 Unique proteins in pal

Entry	Protein names	Gene names	Protein expression
P61204	ADP-ribosylation factor 3	ARF3	Up-regulated
P13473	Lysosome-associated membrane glycoprotein 2 (LAMP-2) (Lysosome-associated membrane protein 2) (CD107 antigen-like family member B) (LGP-96) (CD antigen CD107b)	LAMP2	Up-regulated
P49821	NADH dehydrogenase [ubiquinone] flavoprotein 1, mitochondrial (EC 7.1.1.2) (Complex I-51kD) (CI-51kD) (NADH dehydrogenase flavoprotein	NDUFV1 UQOR1	Up-regulated

	1) (NADH-ubiquinone oxidoreductase 51 kDa subunit)		
Q9NZ01	Very-long-chain enoyl-CoA reductase (EC 1.3.1.93) (Synaptic glycoprotein SC2) (Trans-2,3-enoyl-CoA reductase) (TER)	TECR GPSN2 SC2	Up-regulated
Q9UJU6	Drebrin-like protein (Cervical SH3P7) (Cervical mucin-associated protein) (Drebrin-F) (HPK1-interacting protein of 55 kDa) (HIP-55) (SH3 domain-containing protein 7)	DBNL CMAP SH3P7 PP5423	Up-regulated
P78344	Eukaryotic translation initiation factor 4 gamma 2 (eIF-4-gamma 2) (eIF-4G 2) (eIF4G 2) (Death-associated protein 5) (DAP-5) (p97)	EIF4G2 DAP5 OK/SW-cl.75	Down-regulated
Q9NPA8	Transcription and mRNA export factor ENY2 (Enhancer of yellow 2 transcription factor homolog)	ENY2 DC6	Down-regulated
P61927	60S ribosomal protein L37 (G1.16) (Large ribosomal subunit protein eL37)	RPL37	Down-regulated
O95373	Importin-7 (Imp7) (Ran-binding protein 7) (RanBP7)	IPO7 RANBP7	Down-regulated
Q16204	Coiled-coil domain-containing protein 6 (Papillary thyroid carcinoma-encoded protein) (Protein H4)	CCDC6 D10S170 TST1	Down-regulated
Q13561	Dynactin subunit 2 (50 kDa dynein-associated polypeptide) (Dynactin complex 50 kDa subunit) (DCTN-50) (p50 dynamitin)	DCTN2 DCTN50	Down-regulated
P53621	Coatomer subunit alpha (Alpha-coat protein) (Alpha-COP) (HEP-COP) (HEPCOP) [Cleaved into: Xenin (Xenopsin-related peptide); Proxenin]	COPA	Down-regulated

List of Proteins that are exclusive in the condition of pal vs veh, suggesting that tibolone regulated their expression to a level similar to the vehicle

Weighed Gene Correlation Network Analysis

The unsupervised hierarchical clustering analysis based on protein abundances in the 18 samples showed that the identified differentially expressed proteins can generate a proteomic signature linked to the use of the different treatments or control (Fig. 7). A total of 9 gene modules were generated (blue, yellow, turquoise, pink, red, green, magenta, purple, black, and gray); most of the genes were summarized in the "blue module" (Fig. 7).

According to the module-trait association, the red module had the highest correlation coefficient followed by turquoise and pink, then the 3 modules were selected for further analysis (Fig. 7c). Genetic significance (GS) was used to measure the degree of association between the gene and the trait. Module Membership (MM) was used to determine the location of a global network. GS versus MM reflected the relationship between treatment and genes. The results revealed that the red, pink, and turquoise modules were essential in the responses generated by treatment (Fig. 7F). These proteins generated a total of 355 nodes and 2657 edges and after the MCODE algorithm, it was reduced to 110 hub proteins and 856 edges in different groups (Fig. 8 and supplementary material 7). These proteins, having a high weight in the network with various interactions, are very relevant in the system and may be possible targets for understanding lipotoxic damage and the treatment with tibolone.

Based on the study by Yang (et al. 2019), the proteins with the highest weight in the system were identified, and key proteins were considered as proteins that have a high weight in the network and with very significant differences in differential expression and are of high relevance. Since when they are modified it can seriously disturb the system due to the high number of interactions they have (Yang et al., 2019). Therefore, to define the key proteins, the proteins present in the hubs were intercepted with the differentially expressed proteins with an adjusted p_value or q_value <0.05, to have greater reliability when highlighting the key proteins in the data of this study, obtaining a total of 27 proteins that fulfilled this condition, of which 10 are related to the response induced by the lipotoxic damage generated by pal and 17 to the action of tibolone in human astrocytes (Table 6). It was found that when removing the proteins that were shared between the comparison of tip_vs_veh and pal_vs_veh, and against tip_vs_pal, in pal they remained as exclusive ARF3 up-regulated and IPO7 down-regulated proteins (Table 6) which are related to different diseases, but among them to disorders of the nervous system (Fig. 9).

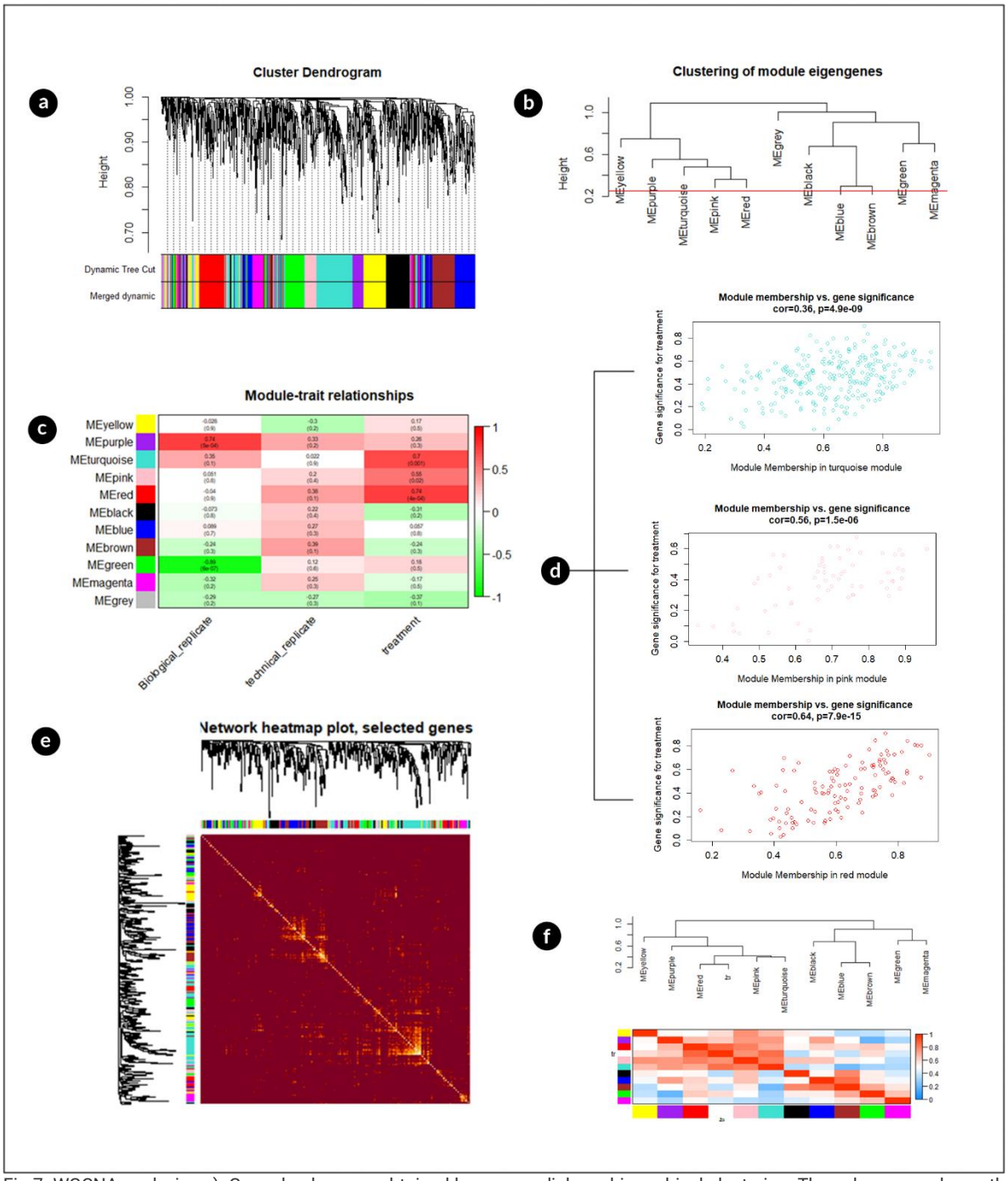

Fig 7. WGCNA analysis: a). Gene dendrogram obtained by average linkage hierarchical clustering. The color row underneath the dendrogram shows the module assignment determined by the Dynamic Tree Cut. b). Heatmap plot of topological overlap in the gene network. In the heatmap, each row and column correspond to a gene, light color denotes low topological overlap, and progressively darker red denotes higher topological overlap. Darker squares along the diagonal correspond to modules. The gene dendrogram and module assignment are shown along the left and top. c). Hierarchical clustering of module eigengenes that summarize the modules found in the clustering analysis. Branches of the dendrogram (the meta-modules) group together eigengenes that are positively correlated. d). Heatmap plot of the adjacencies in the eigengene network including the trait weight. Each row and column in the heatmap correspond to one module eigengene (labeled by color) or weight. In the heatmap, green color represents low adjacency (negative correlation), while red represents high adjacency (positive correlation). Squares of red color along the diagonal are the meta-modules. e). Heath map of the relation between treatment and the different modules f). A scatterplots of gene significance for weight versus module membership (MM) for the modules “red”, “pink” “turquoise”. GS and MM exhibit a very significant correlation, implying that hub genes of these modules also tend to be highly correlated with the treatments.

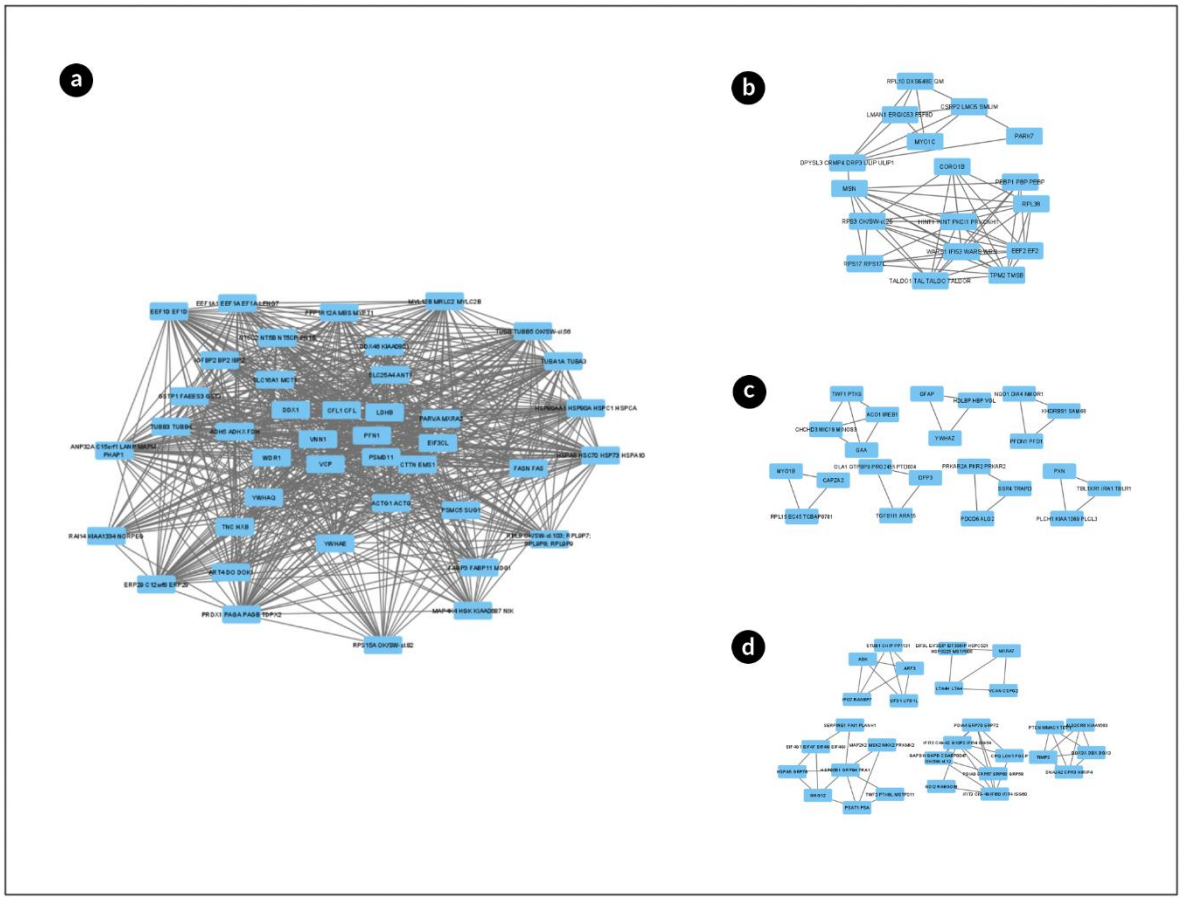

FIG.8 hub-proteins; Protein-protein interaction network with the GeneID, of the highly correlated modules of proteins from WGCNA. Different modules generated in the whole data set- after using the MCODE algorithm of Cytoscape to reduce the nodes for those with more weight in the network reducing from 355 nodes and 2657 edges to 110 nodes and 856 edges

Tabla 6 Key protein

pal_vs_veh Up-regulated	pal_vs_veh Down-regulated	tip_vs_veh Up-regulated	tip_vs_veh Down-regulated	tip_vs_pal Up-regulated	tip_vs_pal Down-regulated
ARF3	ALS2 ALS2CR6 KIAA1563	MAP4K4 HGK KIAA0687 NIK	ALS2 ALS2CR6 KIAA1563	Ninguna	CHCHD3 MIC19 MINOS3

PTEN MMAC1 TEP1	STUB1 CHIP PP1131	PLCH1 KIAA1069 PLCL3	TGFB1I1 ARA55		TGFB1I1 ARA55
	ADK	PDCD6 ALG2	CHCHD3 MIC19 MINOS3		ACO1 IREB1
	DNAJA2 CPR3 HIRIP4	CAPZA2	MYO1B		TWF1 PTK9
	TIMP2	TWF2 PTK9L MSTP011	STUB1 CHIP PP1131		DPP3
	IPO7 RANBP7	PTEN MMAC1 TEP1	EIF4G1 EIF4F EIF4G EIF4GI		OLA1 GTPBP9 PRO2455 PTD004
	UFD1 UFD1L	NT5C2 NT5B NT5CP PNT5	TIMP2		GAA
	MYO1B	CPQ LCH1 PGCP	DNAJA2 CPR3 HIRIP4		
		DDX46 KIAA0801	ADK		

		IFIT3 CIG-49 IFI60 IFIT4 ISG60	TWF1 PTK9		
		VNN1	DDX3X DBX DDX3		
		GNG12	OLA1 GTPBP9 PRO2455 PTD004		
		SLC25A4 ANT1	DPP3		
		IFIT2 CIG-42 G10P2 IFI54 ISG54	RPL15 EC45 TCBAP0781		
			UFD1 UFD1L		
			PSMD11		
			SERPINE1 PAI1 PLANH1		

List of hub proteins that were found in the differentially expressed proteins in each comparison. When buying the hub proteins, intersected with the differentially expressed proteins, we found two hub proteins that are exclusive to pal, ARF3 up-regulated and IPO7 down-regulated.

ARF3

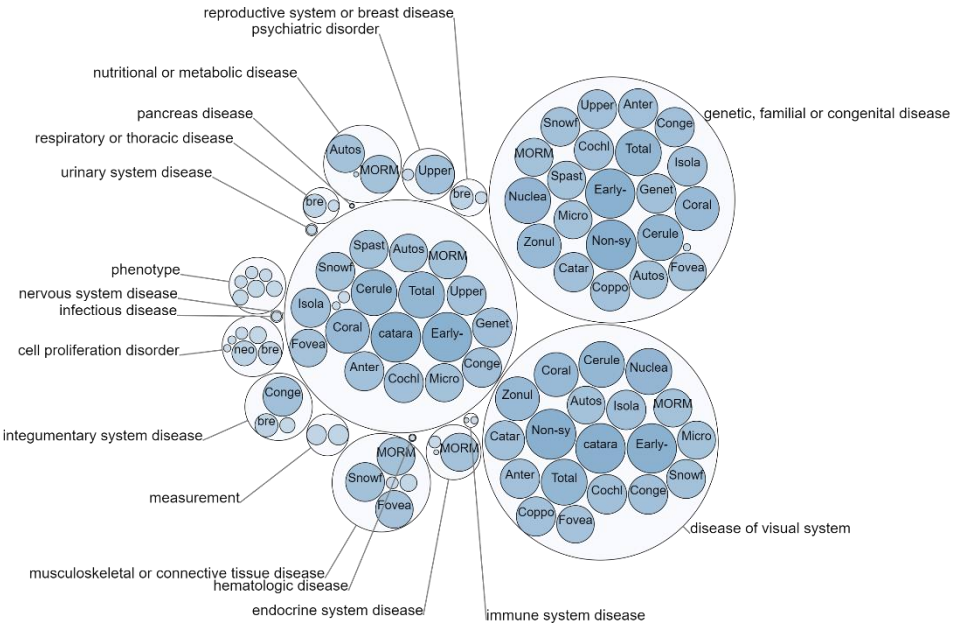

IPO7

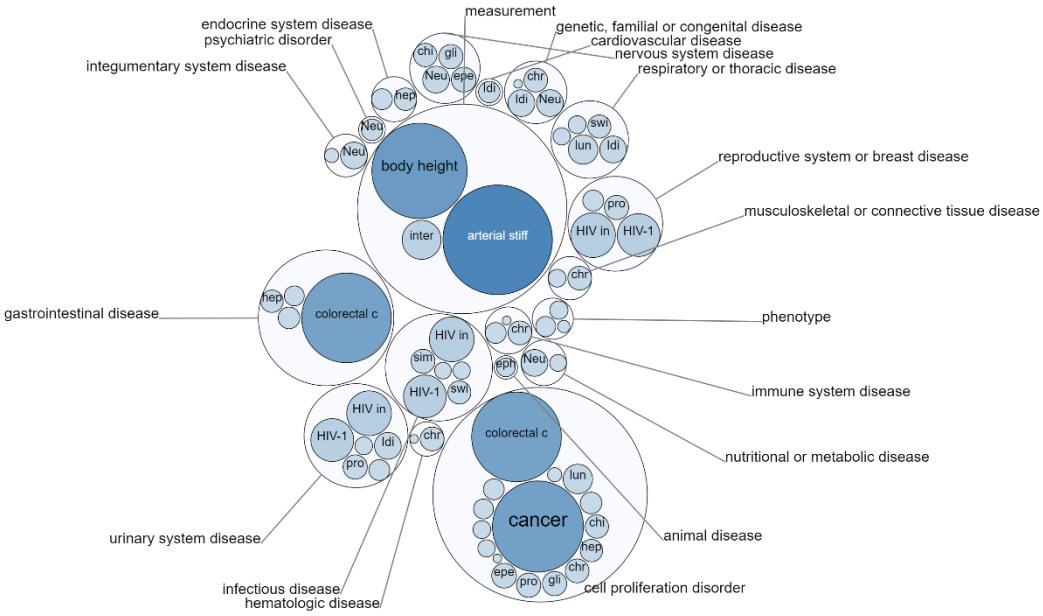

Discussion

The differential expression of proteins exclusively in pal with a high weight in the networks, highlighted two proteins, ARF3 up-regulated and IPO7 down-regulated, which is related to the activation of p53, a characteristic of ribosomal biogenesis stress and increased binding of Mdm2 to ribosomal proteins L5 and L11 (RPL5 and RPL11) (Golomb et al., 2012). Besides, IPO7 depletion affects the transport of other ribosomal proteins such as RPL23A, RPS7, and RPL5, affecting ribosomal biogenesis (Bursac et al., 2014; Golomb et al., 2012). It has been reported in the literature that the depletion of several ribosomal proteins except for RPL5 and RPL 11, induces a response by p53 that generates an inhibition of protein translation and a blockage in the phases of the cell cycle G1 and G2 / M (Fumagalli et al., 2012). This is related to the results obtained because among the proteins negatively regulated by pal is also found the ribosomal protein 60S L37 or RPL37, which would indicate a possible involvement of pal in the protein translation machinery. Of particular interest is the absence of significant differences between tip and veh; in the IPO7 and RPL37 proteins, considering that tip is tibolone with pal, it could mean that tibolone would have a role in the expression of IPO7 and RPL37 at levels similar to those observed with the vehicle, which could be related to its protective effect. This observation agrees with the study by Evans et al., (2019), who, in a mouse model with tauopathy, reported a reduction in the synthesis of ribosomal proteins such as some RPS and RPL (Evans et al., 2019). Additionally, it has been reported that in AD the protein translation machinery is altered, mainly elongation factors and ribosomal proteins (Hernández-Ortega et al., 2016); At the cellular level, the study reports that in the Alzheimer's disease model, astrocytes showed a reduction in ribosomal binding and translation-related proteins (Rocchio et al., 2019). Similarly, reduced protein synthesis has been associated with the progression of PD (Deshpande et al., 2020). This may indicate that pal generates changes like those that can be seen in the progression of some NDs (Deshpande et al., 2020; Rocchio et al., 2019). In addition to the above, it was observed that tibolone reduced the eukaryotic translation initiation factor 4 gamma 1, (Adjibade et al., 2017).

On the other hand, the ARF3 protein that increased in pal vs veh is related to Golgi transport to different regions (Gaudet et al., 2011) and specifically with retrograde transport to the ER (Yu et al., 2014), this shows that it would not only modify the translation of the proteins but also their transport. Additionally, when comparing the lists, pal is found to reduce the expression of dynactin subunit 2 (DCTN2),this is related to the transport from the ER to the Golgi, the formation of the mitotic spindle, and that this subunit interacts directly with the other subunits of the actin (Echeverri et al., 1996; Staples et al., 2014). The above has also been reported on gene and protein functions in NCBI (DCTN2 dynactin subunit 2 [Homo sapiens (human)] - Gene - NCBI). This is interesting because, in a mouse model, was observed that dysfunction in the dynein/dynactin ratio led to the development of

amyotrophic lateral sclerosis (Teuling et al., 2008). Additionally, it has been reported that the overexpression of DCTN2 is harmful, in the transport of motor neurons and leads to the development of neuromotor diseases (De Vos and Hafezparast, 2017; LaMonte et al., 2002). However, in this study, it is down-regulated and the possible effects of down-regulation of DCTN2 in the brain are not clear.

Another protein that is up-regulated only in pal is RuvB-like 1 (EC 3.6.4.12), this protein is responsible for acetylating histones H4 and H2A, activating the transcription of different genes (Doyon et al., 2004), some of these are associated with oncogenes, apoptosis, senescence, or DNA repair (Doyon et al., 2004). Interestingly, this protein is also related to cell proliferation (Gartner et al., 2003). In addition to the proteins related to the inflammatory response, suggested that pal regulates proteins related to gliosis processes, as observed in Liu's study in mouse astrocytes (Liu et al., 2013b); considering that they are unique proteins in the pal treatment, it would mean that tibolone managed to return its expression levels to those of the control. This is consistent with the observed in preliminary reports showing that part of the protective effects of tibolone on astrocytes is related to the regulation of inflammation (Del Río et al., 2020; Osorio et al., 2020).

The results of this study additionally show that among the unique pal proteins up-regulated are the very long chain Enoyl-CoA reductase increases (EC 1.3.1.93), Succinate - CoA ligase beta subunit, mitochondrial (EC 6.2.1.5), and protein 1 for elongation of very long-chain FAs (EC 2.3.1.199), which significantly enrich for fatty acid metabolism and fatty acid elongation. This suggests a relationship between the synthesis of very-long-chain FAs and the synthesis of sphingolipids through the metabolic pathway of sphingosine 1-phosphate (S1P) (Wakashima et al., 2014). The accumulation of a very long-chain FAs in the brain is related to demyelination caused by peroxisomal pathologies (Braverman and Eichler, 2009). On the other hand, the dysfunction of the S1P receptor signaling system gives rise to several vascular defects, such as angiogenesis and increased inflammation due to the increased permeability it generates in the blood vessels (Obinata and Hla, 2019). Although, it should not be stated that the effect of S1P is detrimental since it can have a dual role in the brain, resulting in protection in some conditions and harmful in others (Karunakaran and van Echten-Deckert, 2017). Therefore, it would be interesting to study further what effects S1P is having on human astrocytes under lipotoxic damage with pal.

By focusing on the proteins shared between pal_vs_veh and tip_vs_veh, the SRP68 protein that is part of SRP stands out, that is necessary for the translocation of proteins to the ER (Lakkaraju et al.,

2007). That went from being down-regulated in pal vs veh to up-regulated in tip vs veh. It has been observed that when generating a reconstituted SRP in the absence of the SRP68-SRP72 heterodimer, it lacks elongation and translocation arrest activity (Grotwinkel et al., 2014; Siegel and Walter, 1985). The elongation arrest function is physiologically important in mammalian cells since the efficiency of protein translocation to the ER is significantly reduced when the SRP elongation arrest function is canceled, affecting its function (Lakkaraju et al., 2007; Mary et al., 2010).

Apart from the proteins that tibolone returned to expression levels close to those of the control, it is important to note that some of the differentially expressed proteins in the tip versus pal comparison could explain the protective response of tibolone (Table 3) and (Fig. 6). One of these proteins is the carboxyterminal ubiquitin hydrolase 14 (EC 3.4.19.12), which acts as a physiological inhibitor of ER-associated degradation through interaction with ERN1; According to the above, tibolone could be altering the regulation of autophagy generated by pal in astrocytes (Ortiz-Rodriguez et al., 2018).

When comparing tip against pal, the drebrin-like protein or (DBNL) down-regulated is additionally observed. DBNL binds to actin and plays a role in its polymerization (Gaudet et al., 2011); However, it has also been shown that activates the N-terminal c-Jun kinase (JNK) (Ensenat et al., 1999); This process is related to pro-apoptotic signaling (Dhanasekaran and Reddy, 2008), which indicates that tibolone has a role in its regulation, and this could contribute to the protective response observed in the study by (Martin-Jiménez et al., 2020). In addition to the above, DBNL is also associated with neutrophil degranulation processes, which are related to inflammatory processes (Rocha-Perugini et al., 2017). However, it should be noted that this study suggests that the tibolone response may also be associated with a reduction in the MIC19 subunit of the MICOS complex. Darshi (et al., 2011), show that reduction is associated with changes in mitochondrial morphology (loss of mitochondrial ridges) reducing the efficiency of mitochondria (Darshi et al., 2011).

In the unique proteins that observed in the comparison tip vs veh, the up regulation of IFIT3 (protein induced by interferon with repeats of tetratricopeptide 3). This protein acts as an inhibitor of cellular and viral processes, cell migration, viral proliferation, signaling, and replication (Pichlmair et al., 2011). It has anti-proliferative activity through the positive regulation of the negative regulators of the cell cycle CDKN1A / p21 and CDKN1B / p27. Normally, the turnover of CDKN1B / p27 is regulated by COPS5, which binds CDKN1B / p27 in the nucleus and exports it to the cytoplasm for its ubiquitin-dependent degradation (Xiao et al., 2006). IFIT3 sequesters COPS5 in the cytoplasm, increasing the levels of the nuclear protein CDKN1B / p27. It up-regulates CDKN1A / p21 by down-

regulating MYC, a repressor of CDKN1A / p21 (Xiao et al., 2006). Furthermore, this protein can negatively regulate the proapoptotic effects of IFIT2 (Stawowczyk et al., 2011), a protein that pal increased its expression.

Furthermore, it was also found that mitogen-activated protein kinase 4 (MAP4K4) may play a role in the response to environmental stress and cytokines such as TNF-α (Kaneko et al., 2011). This protein has been shown to play a role in the induction of ARF transduction (Yue et al., 2014)and the negative regulation of apoptosis (Liu et al., 2011). Therefore, MAP4K4 and IFIT3 could be contributing to attenuate the apoptotic processes generated by pal, and IFIT3, in addition, could be preventing excessive proliferation, which is part of the typical astrogliosis process (Garzón et al., 2016; Karki et al., 2014a; Ng and Say, 2018).

In comparison with the vehicle, tibolone increased programmed cell death protein 6, which plays different roles in cell function, such as the regulation of cell proliferation and vesicular transport from ER to Golgi (Okumura et al., 2009), regulating the size of COPII vesicles (McGourty et al., 2016), membrane repair, stabilization of weak protein interactions (Inuzuka et al., 2010; Takeshi et al., 2015), and participates in the acceleration of apoptosis by increasing caspase 3 activity (Lee et al., 2005). However, considering that tibolone reduced cell death in NHA treated with pal (Martin-Jiménez et al., 2020), it is not so likely that in this case, it activates the pro-apoptotic pathway.

On the other hand, tibolone increased the expression of two proteins that regulated actin polymerization and reduced its rapid polymerization, which was the alpha-2 subunit of the F-actin protection protein and Twinfilin-2 (Gaudet et al., 2011). Although, tibolone also reduced Twinfilin-1 which reduces actin polymerization (Gaudet et al., 2011). The above could weigh the inhibitory effect of actin polymerization caused by the alpha-2 or subunit of the protection protein F-actin and Twinfilin-2.

Some of the pathways observed in this study have not been reported as a response to high amounts of saturated fatty acids in astrocytes but have been reported in other types of cells; how the reduction of translation caused by pal in macrophages through the activation of eIF2α, among those IκBα proteins that lead to inflammatory processes (Korbecki and Bajdak-Rusinek, 2019). The results of the present study show that pal reduced the expression of eIF2α, and more importantly, recent findings suggest that phosphorylation of eIF2α does not necessarily lead to down-regulation of global translation and a mandatory connection should not be assumed. Between the negative regulation of translation and

690 the phosphorylation of eIF2α, therefore a down-regulation of eIF2α will not induce an increase in
691 protein translation and therefore the role that eIF2α generates must be validated independently and
692 not solely by its expression or phosphorylation (Boye and Grallert, 2020). On the other hand, it is
693 interesting that mutations in the enzymes responsible for phosphorylating eIF2α lead to human
694 diseases, which often include neurological and/or neurodegenerative pathologies (Moon et al., 2018).
695
696 Although no differentially expressed proteins were found that were directly related to an
697 inflammation response such as NF-κB, the results of this study show that pal up-regulates the proteins
698 related to the transformation of pal to other more complex intermediates such as TERC, ELOVL1,
699 and ACAA1, which are related to the metabolism of FAs and the elongation of very long-chain FAs.
700 This result is interesting because when pal accumulates in the cell it can be transformed into
701 diacylglycerol and ceramides, these can activate several signaling pathways common for
702 lipopolysaccharide-mediated activation of TLR4. It is known that pal metabolic products modulate
703 the activation of various PKCs, ER stress and can cause increased ROS generation (Korbecki and
704 Bajdak-Rusinek, 2019). And even inflammation and cell death if it is about ceramides (Drosatos and
705 Schulze, 2013; Liu et al., 2013b). However, it is not known what type of metabolic products were
706 generated in this study and it would be relevant to compare it with the metabolomic data of pal in
707 NHA cells.
708
709 The damage caused by pal has been reported to trigger the metabolic inflammatory response in
710 astrocytes and is generally associated with damaging mechanisms such as oxidative stress, ER stress,
711 and autophagic defects (Ortiz-Rodriguez et al., 2018; Ortiz-Rodriguez and Arevalo, 2020). In this
712 sense, it has also been reported that tibolone exerts protective functions against inflammation in
713 neuronal experimental models (Del Río et al., 2020). The findings of this study agree with literature
714 reports, except for the expression changes associated with oxidative stress generated by pal, although
715 it should be noted that ROS production by pal in human astrocytes is not so different from control in
716 the study by Martin-Jiménez (et al., 2020) which has the same conditions used in this study. Similarly,
717 it was reported in another study with astrocytes treated with pal 1mM for 24h that there was no ROS
718 production (González-Giraldo et al., 2018). This could be related to mechanisms of damage and cell
719 death generated by pal that are independent of ROS production (Hickson-Bick et al., 2002) and this
720 is probably since pal is not being used by the β-oxidation pathway, but maybe is increasing ceramide
721 synthesis (Blázquez et al., 2001; Patil et al., 2007). Finally, it is important to remember that tibolone
722 must be metabolized and the protective effect in the brain is generated by 3-alpha-hydroxy and 3-

beta-hydroxy-tibolone(Del Río et al., 2020) and this could lead to a dependence on its correct metabolism and the observation of an apparent ambiguous response on the part of tibolone.

Conclusion

This is the first comprehensive study of the proteomic profile of human astrocytes subjected to lipotoxic damage, its results expand our understanding of the lipotoxic effect of palmitic acid on human astrocytes. 110 hub proteins were identified and 27 of them were differentially expressed, of which 10 are related to the response induced by lipotoxic damage generated by palmitic acid and 17 to the action of tibolone in human astrocytes. Among the proteins related to the damage caused by palmitic acid, an association was found with the activation of inflammation, immune response, dysregulation of protein synthesis, autophagy, vesicle transport, and ER-related processes. It was also evidenced that some of the effects generated by palmitic acid such as the reduction of some ribosomal proteins and the dysregulation of protein translation. Interestingly, tibolone returned the expression of several of these proteins to vehicle levels.

Additionally, tibolone reduced the expression of proteins that activate pro-apoptotic pathways. However, the tibolone response has effects that may seem detrimental to the cell, such as a reduction in the expression of aconitase and the MICOS complex or an increase in a protein with pro-apoptotic activity. Therefore, it cannot be said that tibolone completely reverses the damage caused by palmitic acid, but it does show protective effects at the astrocyte level and, in contrast to what has been previously reported, it is likely that the beneficial effects may outweigh the harmful effects promising its use to treat lipotoxic damage in human astrocytes

Conflict of interest

The authors declare no conflict of interest

Acknowledgments

The experiments, and analysis of this study were funded by Minciencias grants 7425, 8845 and 20302 by Pontificia Universidad Javeriana. We want to acknowledge, the proteomics unit of the Complutense University of Madrid, for the training with proteomics datasets. and the UC davis-proteomics core for the proteomics identification service

Bibliography

Acaz-Fonseca, E., Sanchez-Gonzalez, R., Azcoitia, I., Arevalo, M. A., and Garcia-Segura, L. M. (2014). Role of astrocytes in the neuroprotective actions of 17??-estradiol and selective estrogen receptor modulators. *Mol. Cell. Endocrinol.* 389, 48–57. doi:10.1016/j.mce.2014.01.009.

Adjibade, P., Grenier St-Sauveur, V., Bergeman, J., Huot, M. E., Khandjian, E. W., and Mazroui, R. (2017). DDX3 regulates endoplasmic reticulum stress-induced ATF4 expression. *Sci. Rep.* 7. doi:10.1038/s41598-017-14262-7.

Anderson, G., Rodriguez, M., and Reiter, R. J. (2019). Multiple sclerosis: Melatonin, orexin, and ceramide interact with platelet activation coagulation factors and gut-microbiome-derived butyrate in the circadian dysregulation of mitochondria in glia and immune cells. *Int. J. Mol. Sci.* 20. doi:10.3390/ijms20215500.

Arevalo, M. A., Santos-Galindo, M., Lagunas, N., Azcoitia, I., and Garcia-Segura, L. M. (2011). Selective estrogen receptor modulators as brain therapeutic agents. *J. Mol. Endocrinol.* 46. doi:10.1677/JME-10-0122.

Ávila Rodriguez, M., Garcia-Segura, L. M., Cabezas, R., Torrente, D., Capani, F., Gonzalez, J., et al. (2014). Tibolone protects T98G cells from glucose deprivation. *J. Steroid Biochem. Mol. Biol.* 144, 294–303. doi:10.1016/j.jsbmb.2014.07.009.

Bazinet, R. P., and Layé, S. (2014). Polyunsaturated fatty acids and their metabolites in brain function and disease. *Nat. Rev. Neurosci.* 15, 771. Available at: http://dx.doi.org/10.1038/nrn3820.

Bentsen, H. (2017). Dietary polyunsaturated fatty acids, brain function and mental health. *Microb. Ecol. Health Dis.* 28, 1281916. doi:10.1080/16512235.2017.1281916.

Blázquez, C., Geelen, M. J., Velasco, G., and Guzmán, M. (2001). The AMP-activated protein kinase prevents ceramide synthesis de novo and apoptosis in astrocytes. *FEBS Lett.* 489, 149–153. doi:10.1016/s0014-5793(01)02089-0.

Boye, E., and Grallert, B. (2020). eIF2α phosphorylation and the regulation of translation. *Curr. Genet.* 66, 293–297. doi:10.1007/s00294-019-01026-1.

Braverman, N., and Eichler, F. (2009). “Peroxisomal Disorders and Neurological Disease,” in, ed. L. R. B. T.-E. of N. Squire (Oxford: Academic Press), 579–588. doi:https://doi.org/10.1016/B978-008045046-9.02011-8.

Bursac, S., Brdovcak, M. C., Donati, G., and Volarevic, S. (2014). Activation of the tumor suppressor p53 upon impairment of ribosome biogenesis. *Biochim. Biophys. Acta - Mol. Basis Dis.* 1842, 817–830. doi:https://doi.org/10.1016/j.bbadis.2013.08.014.

Cakir, I., and Nillni, E. A. (2019). Endoplasmic Reticulum Stress, the Hypothalamus, and Energy Balance. *Trends Endocrinol. Metab.* 30, 163–176. doi:10.1016/j.tem.2019.01.002.

Carta, G., Murru, E., Banni, S., and Manca, C. (2017). Palmitic Acid: Physiological Role, Metabolism and Nutritional Implications . *Front. Physiol.* 8, 902. Available at: https://www.frontiersin.org/article/10.3389/fphys.2017.00902.

Chai, L. E., Law, C. K., Mohamad, M. S., Chong, C. K., Choon, Y. W., Deris, S., et al. (2014). Investigating the effects of imputation methods for modelling gene networks using a dynamic bayesian network from gene expression data. *Malays. J. Med. Sci.* 21, 20–27. Available at: https://pubmed.ncbi.nlm.nih.gov/24876803.

Chen, L. N., Wang, Y., Ma, D. L., and Chen, Y. Y. (2006). Short interfering RNA against the PDCD5 attenuates cell apoptosis and caspase-3 activity induced by Bax overexpression. *Apoptosis* 11, 101–111. doi:10.1007/s10495-005-3134-y.

Darshi, M., Mendiola, V. L., Mackey, M. R., Murphy, A. N., Koller, A., Perkins, G. A., et al. (2011). ChChd3, an inner mitochondrial membrane protein, is essential for maintaining Crista integrity and mitochondrial function. *J. Biol. Chem.* 286, 2918–2932. doi:10.1074/jbc.M110.171975.

De Aguilar, J. L. G., and González De Aguilar, J.-L. (2019). Lipid Biomarkers for Amyotrophic Lateral Sclerosis. *Front. Neurol.* 10, 284. doi:10.3389/fneur.2019.00284.

De Vos, K. J., and Hafezparast, M. (2017). Neurobiology of axonal transport defects in motor neuron diseases: Opportunities for translational research? *Neurobiol. Dis.* 105, 283–299. doi:10.1016/j.nbd.2017.02.004.

Del Río, J. P., Molina, S., Hidalgo-Lanussa, O., Garcia-Segura, L. M., and Barreto, G. E. (2020). Tibolone as Hormonal Therapy and Neuroprotective Agent. *Trends Endocrinol. Metab.* 31, 742–759. doi:10.1016/j.tem.2020.04.007.

Deshpande, P., Flinkman, D., Hong, Y., Goltseva, E., Siino, V., Sun, L., et al. (2020). Protein synthesis is suppressed in sporadic and familial Parkinson's disease by LRRK2. *FASEB J.* n/a. doi:10.1096/fj.202001046R.

Dhanasekaran, D. N., and Reddy, E. P. (2008). JNK signaling in apoptosis. *Oncogene* 27, 6245–6251. doi:10.1038/onc.2008.301.

Doyon, Y., Selleck, W., Lane, W. S., Tan, S., and Côté, J. (2004). Structural and Functional Conservation of the NuA4 Histone Acetyltransferase Complex from Yeast to Humans. *Mol. Cell. Biol.* 24, 1884–1896. doi:10.1128/mcb.24.5.1884-1896.2004.

Dozio, V., and Sanchez, J. C. (2018). Profiling the proteomic inflammatory state of human astrocytes using DIA mass spectrometry 06 Biological Sciences 0601 Biochemistry and Cell

825 Biology. *J. Neuroinflammation* 15, 331. doi:10.1186/s12974-018-1371-6.
826 Drosatos, K., and Schulze, P. C. (2013). Cardiac Lipotoxicity: Molecular Pathways and Therapeutic
827 Implications. *Curr. Heart Fail. Rep.* 10, 109–121. doi:10.1007/s11897-013-0133-0.
828 Echeverri, C. J., Paschal, B. M., Vaughan, K. T., and Vallee, R. B. (1996). Molecular
829 characterization of the 50-kD subunit of dynactin reveals function for the complex in
830 chromosome alignment and spindle organization during mitosis. *J. Cell Biol.* 132, 617–633.
831 doi:10.1083/jcb.132.4.617.
832 Elo, L. L., Filen, S., Lahesmaa, R., and Aittokallio, T. (2008). Reproducibility-optimized test
833 statistic for ranking genes in microarray studies. *IEEE/ACM Trans. Comput. Biol. Bioinforma.*
834 5, 423–431. doi:10.1109/tcbb.2007.1078.
835 Ensenat, D., Yao, Z., Wang, X. S., Kori, R., Zhou, G., Lee, S. C., et al. (1999). A novel Src
836 homology 3 domain-containing adaptor protein, HIP-55, that interacts with hematopoietic
837 progenitor kinase 1. *J. Biol. Chem.* 274, 33945–33950. doi:10.1074/jbc.274.48.33945.
838 Evans, H. T., Benetatos, J., van Roijen, M., Bodea, L. L.-G., and Götz, J. (2019). Decreased
839 synthesis of ribosomal proteins in tauopathy revealed by non-canonical amino acid labelling.
840 *EMBO J.* 38, e101174. doi:10.15252/embj.2018101174.
841 Fumagalli, S., Ivanenkov, V. V, Teng, T., and Thomas, G. (2012). Suprainduction of p53 by
842 disruption of 40S and 60S ribosome biogenesis leads to the activation of a novel G2/M
843 checkpoint. *Genes Dev.* 26, 1028–1040. doi:10.1101/gad.189951.112.
844 Gartner, W., Rossbacher, J., Zierhut, B., Daneva, T., Base, W., Weissel, M., et al. (2003). The ATP-
845 dependent helicase RUVBL1/TIP49a associates with tubulin during mitosis. *Cell Motil.*
846 *Cytoskeleton* 56, 79–93. doi:10.1002/cm.10136.
847 Garzón, D., Cabezas, R., Vega, N., Ávila-Rodriguez, M., Gonzalez, J., G??mez, R. M., et al.
848 (2016). Novel Approaches in Astrocyte Protection: from Experimental Methods to
849 Computational Approaches. *J. Mol. Neurosci.* 58, 483–492. doi:10.1007/s12031-016-0719-6.
850 Gaudet, P., Livstone, M. S., Lewis, S. E., and Thomas, P. D. (2011). Phylogenetic-based
851 propagation of functional annotations within the Gene Ontology consortium. *Brief.*
852 *Bioinform.* 12, 449–462. doi:10.1093/bib/bbr042.
853 Golomb, L., Bublik, D. R., Wilder, S., Nevo, R., Kiss, V., Grabusic, K., et al. (2012). Importin 7
854 and exportin 1 Link c-Myc and p53 to regulation of ribosomal Biogenesis. *Mol. Cell* 45, 222–
855 232. doi:10.1016/j.molcel.2011.11.022.
856 González-Giraldo, Y., Garcia-Segura, L. M., Echeverria, V., and Barreto, G. E. (2018). Tibolone
857 Preserves Mitochondrial Functionality and Cell Morphology in Astrocytic Cells Treated with
858 Palmitic Acid. *Mol. Neurobiol.* 55, 4453–4462. doi:10.1007/s12035-017-0667-3.

Grotwinkel, J. T., Wild, K., Segnitz, B., and Sinning, I. (2014). SRP RNA remodeling by SRP68 explains its role in protein translocation. *Science (80-.).* 344, 101–104. doi:10.1126/science.1249094.

Gupta, S., Knight, A. G., Gupta, S., Keller, J. N., and Bruce-Keller, A. J. (2012). Saturated long-chain fatty acids activate inflammatory signaling in astrocytes. *J. Neurochem.* 120, 1060–1071. doi:10.1111/j.1471-4159.2012.07660.x.

He, Y., Zhou, L., Fan, Z., Liu, S., and Fang, W. (2018). Palmitic acid, but not high-glucose, induced myocardial apoptosis is alleviated by N-acetylcysteine due to attenuated mitochondrial-derived ROS accumulation-induced endoplasmic reticulum stress. *Cell Death Dis.* 9, 568. doi:10.1038/s41419-018-0593-y.

Hernández-Ortega, K., Garcia-Esparcia, P., Gil, L., Lucas, J. J., and Ferrer, I. (2016). Altered Machinery of Protein Synthesis in Alzheimer's: From the Nucleolus to the Ribosome. *Brain Pathol.* 26, 593–605. doi:10.1111/bpa.12335.

Hickson-Bick, D. L. M., Sparagna, G. C., Buja, L. M., and McMillin, J. B. (2002). Palmitate-induced apoptosis in neonatal cardiomyocytes is not dependent on the generation of ROS. *Am. J. Physiol. Circ. Physiol.* 282, H656–H664. doi:10.1152/ajpheart.00726.2001.

Huber, W., von Heydebreck, A., Sültmann, H., Poustka, A., and Vingron, M. (2002). Variance stabilization applied to microarray data calibration and to the quantification of differential expression. *Bioinformatics* 18 Suppl 1, S96-104. doi:10.1093/bioinformatics/18.suppl_1.s96.

Innis, S. M. (2016). Palmitic Acid in Early Human Development. *Crit. Rev. Food Sci. Nutr.* 56, 1952–1959. doi:10.1080/10408398.2015.1018045.

Inuzuka, T., Suzuki, H., Kawasaki, M., Shibata, H., Wakatsuki, S., and Maki, M. (2010). Molecular basis for defect in Alix-binding by alternatively spliced isoform of ALG-2 (ALG-2GF122) and structural roles of F122 in target recognition. *BMC Struct. Biol.* 10. doi:10.1186/1472-6807-10-25.

Jäkel, S., Albig, W., Kutay, U., Bischoff, F. R., Schwamborn, K., Doenecke, D., et al. (1999). The importin beta/importin 7 heterodimer is a functional nuclear import receptor for histone H1. *EMBO J.* 18, 2411–2423. doi:10.1093/emboj/18.9.2411.

Jäkel, S., and Görlich, D. (1998). Importin beta, transportin, RanBP5 and RanBP7 mediate nuclear import of ribosomal proteins in mammalian cells. *EMBO J.* 17, 4491–4502. doi:10.1093/emboj/17.15.4491.

Kaneko, S., Chena, X., Lua, P., Yao, X., Wright, T. G., Rajurkar, M., et al. (2011). Smad inhibition by the Ste20 kinase misshapen. *Proc. Natl. Acad. Sci. U. S. A.* 108, 11127–11132. doi:10.1073/pnas.1104128108.

Kar, A. N., MacGibeny, M. A., Gervasi, N. M., Gioio, A. E., and Kaplan, B. B. (2013). Intra-axonal synthesis of eukaryotic translation initiation factors regulates local protein synthesis and axon growth in rat sympathetic neurons. *J. Neurosci.* 33, 7165–7174. doi:10.1523/JNEUROSCI.2040-12.2013.

Karki, P., Smith, K., Johnson, J., and Lee, E. (2014a). Astrocyte-derived growth factors and estrogen neuroprotection: Role of transforming growth factor-?? in estrogen-induced upregulation of glutamate transporters in astrocytes. *Mol. Cell. Endocrinol.* 389, 58–64. doi:10.1016/j.mce.2014.01.010.

Karki, P., Webb, A., Zerguine, A., Choi, J., Son, D. S., and Lee, E. (2014b). Mechanism of raloxifene-induced upregulation of glutamate transporters in rat primary astrocytes. *Glia* 62, 1270–1283. doi:10.1002/glia.22679.

Karpievitch, Y. V., Dabney, A. R., and Smith, R. D. (2012). Normalization and missing value imputation for label-free LC-MS analysis. *BMC Bioinformatics* 13 Suppl 1. doi:10.1186/1471-2105-13-S16-S5.

Karunakaran, I., and van Echten-Deckert, G. (2017). Sphingosine 1-phosphate – A double edged sword in the brain. *Biochim. Biophys. Acta - Biomembr.* 1859, 1573–1582. doi:10.1016/j.bbamem.2017.03.008.

Kloosterboer, H. J. (2004). Tissue-selectivity: The mechanism of action of tibolone. *Maturitas* 48, 30–40. doi:10.1016/j.maturitas.2004.02.012.

Korbecki, J., and Bajdak-Rusinek, K. (2019). The effect of palmitic acid on inflammatory response in macrophages: an overview of molecular mechanisms. *Inflamm. Res.* 68, 915–932. doi:10.1007/s00011-019-01273-5.

Lakkaraju, A. K. K., Luyet, P. P., Parone, P., Falguières, T., and Strub, K. (2007). Inefficient targeting to the endoplasmic reticulum by the signal recognition particle elicits selective defects in post-ER membrane trafficking. *Exp. Cell Res.* 313, 834–847. doi:10.1016/j.yexcr.2006.12.003.

LaMonte, B. H., Wallace, K. E., Holloway, B. A., Shelly, S. S., Ascaño, J., Tokito, M., et al. (2002). Disruption of dynein/dynactin inhibits axonal transport in motor neurons causing late-onset progressive degeneration. *Neuron* 34, 715–727. doi:10.1016/S0896-6273(02)00696-7.

Lee, J. H., Rho, S. B., and Chun, T. (2005). Programmed cell death 6 (PDCD6) protein interacts with death-associated protein kinase 1 (DAPk1): Additive effect on apoptosis via caspase-3 dependent pathway. *Biotechnol. Lett.* 27, 1011–1015. doi:10.1007/s10529-005-7869-x.

Liddelow, S. A., and Sofroniew, M. V. (2019). Astrocytes usurp neurons as a disease focus. *Nat. Neurosci.* 22, 512–513. doi:10.1038/s41593-019-0367-6.

927 Liu, A. W., Cai, J., Zhao, X. L., Jiang, T. H., He, T. F., Fu, H. Q., et al. (2011). ShRNA-targeted
928 MAP4K4 inhibits hepatocellular carcinoma growth. *Clin. Cancer Res.* 17, 710–720.
929 doi:10.1158/1078-0432.CCR-10-0331.
930 Liu, B., and Qian, S.-B. (2014). Translational reprogramming in cellular stress response. *Wiley*
931 *Interdiscip. Rev. RNA* 5, 301–315. doi:10.1002/wrna.1212.
932 Liu, L., Martin, R., and Chan, C. (2013a). Palmitate-activated astrocytes via serine
933 palmitoyltransferase increase BACE1 in primary neurons by sphingomyelinases. *Neurobiol.*
934 *Aging* 34, 540–550. doi:https://doi.org/10.1016/j.neurobiolaging.2012.05.017.
935 Liu, L., Martin, R., Kohler, G., and Chan, C. (2013b). Palmitate induces transcriptional regulation
936 of BACE1 and presenilin by STAT3 in neurons mediated by astrocytes. *Exp. Neurol.* 248,
937 482–490. doi:10.1016/j.expneurol.2013.08.004.
938 Liu, M., Kelley, M. H., Herson, P. S., and Hurn, P. D. (2010). Neuroprotection of sex steroids.
939 *Minerva Endocrinol.* 35, 127–143. doi:10.1016/j.jaac.2010.01.025.Measured.
940 Lopez-Rodriguez, A. B., Ávila-Rodriguez, M., Vega-vela, N. E., Capani, F., Gonzalez, J., Garciá-
941 Segura, L. M., et al. (2015). *Estrogen effects on traumatic brain injury*.
942 Lopez-rodriguez, A. B., Marco, A., and Vega-vela, N. E. (2011). Neuroprotection by Exogenous
943 Estrogenic Compounds. doi:10.1016/B978-0-12-801479-0.00006-1.
944 Lushchak, O. V., Piroddi, M., Galli, F., and Lushchak, V. I. (2014). Aconitase post-translational
945 modification as a key in linkage between Krebs cycle, iron homeostasis, redox signaling, and
946 metabolism of reactive oxygen species. *Redox Rep.* 19, 8–15.
947 doi:10.1179/1351000213Y.0000000073.
948 Martin-Jiménez, C., González, J., Vesga, D., Aristizabal, A., and Barreto, G. E. (2020). Tibolone
949 Ameliorates the Lipotoxic Effect of Palmitic Acid in Normal Human Astrocytes. *Neurotox.*
950 *Res.* doi:10.1007/s12640-020-00247-4.
951 Mary, C., Scherrer, A., Huck, L., Lakkaraju, A. K. K., Thomas, Y., Johnson, A. E., et al. (2010).
952 Residues in SRP9/14 essential for elongation arrest activity of the signal recognition particle
953 define a positively charged functional domain on one side of the protein. *RNA* 16, 969–979.
954 doi:10.1261/rna.2040410.
955 McGourty, C. A., Akopian, D., Walsh, C., Gorur, A., Werner, A., Schekman, R., et al. (2016).
956 Regulation of the CUL3 Ubiquitin Ligase by a Calcium-Dependent Co-adaptor. *Cell* 167, 525-
957 538.e14. doi:10.1016/j.cell.2016.09.026.
958 Mikami, S., Masutani, M., Sonenberg, N., Yokoyama, S., and Imataka, H. (2006). An efficient
959 mammalian cell-free translation system supplemented with translation factors. *Protein Expr.*
960 *Purif.* 46, 348–357. doi:10.1016/j.pep.2005.09.021.

961 Moon, S. L., Sonenberg, N., and Parker, R. (2018). Neuronal Regulation of eIF2α; Function in
962 Health and Neurological Disorders. *Trends Mol. Med.* 24, 575–589.
963 doi:10.1016/j.molmed.2018.04.001.
964 Ng, Y. W., and Say, Y. H. (2018). Palmitic acid induces neurotoxicity and gliatoxicity in SH-SY5Y
965 human neuroblastoma and T98G human glioblastoma cells. *PeerJ* 6, e4696–e4696.
966 doi:10.7717/peerj.4696.
967 Obinata, H., and Hla, T. (2019). Sphingosine 1-phosphate and inflammation. *Int. Immunol.* 31, 617–
968 625. doi:10.1093/intimm/dxz037.
969 Odintsova, T. I., Müller, E.-C., Ivanov, A. V, Egorov, T. A., Bienert, R., Vladimirov, S. N., et al.
970 (2003). Characterization and analysis of posttranslational modifications of the human large
971 cytoplasmic ribosomal subunit proteins by mass spectrometry and Edman sequencing. *J.*
972 *Protein Chem.* 22, 249–258. doi:10.1023/a:1025068419698.
973 Okumura, M., Ichioka, F., Kobayashi, R., Suzuki, H., Yoshida, H., Shibata, H., et al. (2009). Penta-
974 EF-hand protein ALG-2 functions as a Ca2+-dependent adaptor that bridges Alix and
975 TSG101. *Biochem. Biophys. Res. Commun.* 386, 237–241. doi:10.1016/j.bbrc.2009.06.015.
976 Okun, E., Griffioen, K. J., Lathia, J. D., Tang, S.-C., Mattson, M. P., and Arumugam, T. V (2009).
977 Toll-like receptors in neurodegeneration. *Brain Res. Rev.* 59, 278–292.
978 doi:10.1016/j.brainresrev.2008.09.001.
979 Ortiz-Rodriguez, A., Acaz-Fonseca, E., Boya, P., Arevalo, M. A., and Garcia-Segura, L. M. (2018).
980 Lipotoxic Effects of Palmitic Acid on Astrocytes Are Associated with Autophagy Impairment.
981 *Mol. Neurobiol.* doi:10.1007/s12035-018-1183-9.
982 Ortiz-Rodriguez, A., and Arevalo, M. A. (2020). The contribution of astrocyte autophagy to
983 systemic metabolism. *Int. J. Mol. Sci.* 21. doi:10.3390/ijms21072479.
984 Osorio, D., Pinzón, A., Martín-Jiménez, C., Barreto, G. E., and González, J. (2020). Multiple
985 Pathways Involved in Palmitic Acid-Induced Toxicity: A System Biology Approach. *Front.*
986 *Neurosci.* 13, 1–14. doi:10.3389/fnins.2019.01410.
987 Patil, S., Melrose, J., and Chan, C. (2007). Involvement of astroglial ceramide in palmitic acid-
988 induced Alzheimer-like changes in primary neurons. *Eur. J. Neurosci.* 26, 2131–2141.
989 doi:10.1111/j.1460-9568.2007.05797.x.
990 Pekny, M., and Pekna, M. (2014). Astrocyte Reactivity and Reactive Astrogliosis: Costs and
991 Benefits. *Physiol. Rev.* 94. doi:10.1152/physrev.00041.2013.
992 Pichlmair, A., Lassnig, C., Eberle, C. A., Górna, M. W., Baumann, C. L., Burkard, T. R., et al.
993 (2011). IFIT1 is an antiviral protein that recognizes 5′-triphosphate RNA. *Nat. Immunol.* 12,
994 624–630. doi:10.1038/ni.2048.

Quijano, C., Trujillo, M., Castro, L., and Trostchansky, A. (2016). Interplay between oxidant species and energy metabolism. *Redox Biol.* 8, 28–42. doi:https://doi.org/10.1016/j.redox.2015.11.010.

Raudvere, U., Kolberg, L., Kuzmin, I., Arak, T., Adler, P., Peterson, H., et al. (2019). G:Profiler: A web server for functional enrichment analysis and conversions of gene lists (2019 update). *Nucleic Acids Res.* 47, W191–W198. doi:10.1093/nar/gkz369.

Reimand, J., Isserlin, R., Voisin, V., Kucera, M., Tannus-Lopes, C., Rostamianfar, A., et al. (2019). Pathway enrichment analysis and visualization of omics data using g:Profiler, GSEA, Cytoscape and EnrichmentMap. *Nat. Protoc.* 14, 482–517. doi:10.1038/s41596-018-0103-9.

Rocchio, F., Tapella, L., Manfredi, M., Chisari, M., Ronco, F., Ruffinatti, F. A., et al. (2019). Gene expression, proteome and calcium signaling alterations in immortalized hippocampal astrocytes from an Alzheimer's disease mouse model. *Cell Death Dis.* 10, 24. doi:10.1038/s41419-018-1264-8.

Rocha-Perugini, V., Gordon-Alonso, M., and Sánchez-Madrid, F. (2017). "Role of drebrin at the immunological synapse," in *Advances in Experimental Medicine and Biology* (Springer New York LLC), 271–280. doi:10.1007/978-4-431-56550-5_15.

Roig-Zamboni, V., Cobucci-Ponzano, B., Iacono, R., Ferrara, M. C., Germany, S., Bourne, Y., et al. (2017). Structure of human lysosomal acid α-glucosidase-a guide for the treatment of Pompe disease. *Nat. Commun.* 8, 1111. doi:10.1038/s41467-017-01263-3.

Shamim, A., Mahmood, T., Ahsan, F., Kumar, A., and Bagga, P. (2018). Lipids: An insight into the neurodegenerative disorders. *Clin. Nutr. Exp.* 20, 1–19. doi:https://doi.org/10.1016/j.yclnex.2018.05.001.

Shang, Y., Xu, X., Duan, X., Guo, J., Wang, Y., Ren, F., et al. (2014). Hsp70 and Hsp90 oppositely regulate TGF-β signaling through CHIP/Stub1. *Biochem. Biophys. Res. Commun.* 446, 387–392. doi:10.1016/j.bbrc.2014.02.124.

Siegel, V., and Walter, P. (1985). Elongation arrest is not a prerequisite for secretory protein translocation across the microsomal membrane. *J. Cell Biol.* 100, 1913–1921. doi:10.1083/jcb.100.6.1913.

Slobodin, B., Han, R., Calderone, V., Vrielink, J. A. F. O., Loayza-Puch, F., Elkon, R., et al. (2017). Transcription Impacts the Efficiency of mRNA Translation via Co-transcriptional N6-adenosine Methylation. *Cell* 169, 326-337.e12. doi:10.1016/j.cell.2017.03.031.

Sofroniew, M. V (2015). Astrocyte barriers to neurotoxic inflammation. *Nat. Rev. Neurosci.* 16. doi:10.1038/nrn3898.

Sorensen, T. I. A., Virtue, S., and Vidal-Puig, A. (2010). Obesity as a clinical and public health

problem: Is there a need for a new definition based on lipotoxicity effects? *Biochim. Biophys. Acta - Mol. Cell Biol. Lipids* 1801, 400–404. doi:10.1016/j.bbalip.2009.12.011.

Staples, C. J., Myers, K. N., Beveridge, R. D. D., Patil, A. A., Howard, A. E., Barone, G., et al. (2014). Ccdc13 is a novel human centriolar satellite protein required for ciliogenesis and genome stability. *J. Cell Sci.* 127, 2910–2919. doi:10.1242/jcs.147785.

Stawowczyk, M., Van Scoy, S., Kumar, K. P., and Reich, N. C. (2011). The interferon stimulated gene 54 promotes apoptosis. *J. Biol. Chem.* 286, 7257–7266. doi:10.1074/jbc.M110.207068.

Suomi, T., Seyednasrollah, F., Jaakkola, M. K., Faux, T., and Elo, L. L. (2017). ROTS: An R package for reproducibility-optimized statistical testing. *PLoS Comput. Biol.* 13, 1–10. doi:10.1371/journal.pcbi.1005562.

Takeshi, T., Kojima, K., Zhang, W., Sasaki, K., Ito, M., Suzuki, H., et al. (2015). Structural analysis of the complex between Penta-Ef-Hand Alg-2 protein and sec31a peptide reveals a novel target recognition mechanism of Alg-2. *Int. J. Mol. Sci.* 16, 3677–3699. doi:10.3390/ijms16023677.

Teuling, E., van Dis, V., Wulf, P. S., Haasdijk, E. D., Akhmanova, A., Hoogenraad, C. C., et al. (2008). A novel mouse model with impaired dynein/dynactin function develops amyotrophic lateral sclerosis (ALS)-like features in motor neurons and improves lifespan in SOD1-ALS mice. *Hum. Mol. Genet.* 17, 2849–2862. doi:10.1093/hmg/ddn182.

Tracey, T. J., Steyn, F. J., Wolvetang, E. J., and Ngo, S. T. (2018). Neuronal Lipid Metabolism: Multiple Pathways Driving Functional Outcomes in Health and Disease. *Front. Mol. Neurosci.* 11, 10. doi:10.3389/fnmol.2018.00010.

Unger, R. H., Clark, G. O., Scherer, P. E., and Orci, L. (2010). Lipid homeostasis, lipotoxicity and the metabolic syndrome. *Biochim. Biophys. Acta - Mol. Cell Biol. Lipids* 1801, 209–214. doi:10.1016/j.bbalip.2009.10.006.

Välikangas, T., Suomi, T., and Elo, L. L. (2017). A comprehensive evaluation of popular proteomics software workflows for label-free proteome quantification and imputation. *Brief. Bioinform.* 19, 1344–1355. doi:10.1093/bib/bbx054.

van Horssen, J., van Schaik, P., and Witte, M. (2019). Inflammation and mitochondrial dysfunction: A vicious circle in neurodegenerative disorders? *Neurosci. Lett.* 710, 132931. doi:https://doi.org/10.1016/j.neulet.2017.06.050.

Wakashima, T., Abe, K., and Kihara, A. (2014). Dual functions of the trans-2-enoyl-CoA reductase TER in the sphingosine 1-phosphate metabolic pathway and in fatty acid elongation. *J. Biol. Chem.* 289, 24736–24748. doi:10.1074/jbc.M114.571869.

World Health Organization (2016). Obesity and overweight. Available at:

http://www.who.int/mediacentre/factsheets/fs311/en/.

World Health Organization (2020). Obesity. Available at: https://www.who.int/news-room/facts-in-pictures/detail/6-facts-on-obesity [Accessed November 10, 2020].

Xiao, S., Li, B., Zhu, H. Q., Song, M. G., Pan, X. R., Jia, P. M., et al. (2006). RIG-G as a key of the antiproliferative activity of interferon-related pathways through enhancing p21 and p27 proteins. *Proc. Natl. Acad. Sci. U. S. A.* 103, 16448–16453. doi:10.1073/pnas.0607830103.

Yang, W., Shi, J., Zhou, Y., Liu, T., Zhan, F., Zhang, K., et al. (2019). Integrating proteomics and transcriptomics for the identification of potential targets in early colorectal cancer. *Int. J. Oncol.* 55, 439–450. doi:10.3892/ijo.2019.4833.

Yu, J., Chia, J., Canning, C. A., Jones, C. M., Bard, F. A., and Virshup, D. M. (2014). WLS Retrograde transport to the endoplasmic reticulum during Wnt secretion. *Dev. Cell* 29, 277–291. doi:10.1016/j.devcel.2014.03.016.

Yue, J., Xie, M., Gou, X., Lee, P., Schneider, M. D., and Wu, X. (2014). Microtubules Regulate Focal Adhesion Dynamics through MAP4K4. *Dev. Cell* 31, 572–585. doi:10.1016/j.devcel.2014.10.025.

Zhao, Y., Lang, G., Ito, S., Bonnet, J., Metzger, E., Sawatsubashi, S., et al. (2008). A TFTC/STAGA module mediates histone H2A and H2B deubiquitination, coactivates nuclear receptors, and counteracts heterochromatin silencing. *Mol. Cell* 29, 92–101. doi:10.1016/j.molcel.2007.12.011.

Supplementary material

Supplementary material 1. Full list of differentially expressed proteins in the comparison between pal_vs_veh

Entry	Protein names	Gene names	Protein expression
P31949	Protein S100-A11 (Calgizzarin) (Metastatic lymph node gene 70 protein) (MLN 70) (Protein S100-C) (S100 calcium-binding protein A11) [Cleaved into: Protein S100-A11, N-terminally processed]	S100A11 MLN70 S100C	Up-regulated
Q9P2R7	Succinate--CoA ligase [ADP-forming] subunit beta, mitochondrial (EC 6.2.1.5) (ATP-specific succinyl-CoA synthetase subunit beta) (A-SCS) (Succinyl-CoA synthetase beta-A chain) (SCS-betaA)	SUCLA2	Up-regulated
Q12904	Aminoacyl tRNA synthase complex-interacting multifunctional protein 1 (Multisynthase complex auxiliary component	AIMP1 EMAP2 SCYE1	Up-regulated

	p43) [Cleaved into: Endothelial monocyte-activating polypeptide 2 (EMAP-2) (Endothelial monocyte-activating polypeptide II) (EMAP-II) (Small inducible cytokine subfamily E member 1)]		
Q9Y265	RuvB-like 1 (EC 3.6.4.12) (49 kDa TATA box-binding protein-interacting protein) (49 kDa TBP-interacting protein) (54 kDa erythrocyte cytosolic protein) (ECP-54) (INO80 complex subunit H) (Nuclear matrix protein 238) (NMP 238) (Pontin 52) (TIP49a) (TIP60-associated protein 54-alpha) (TAP54-alpha)	RUVBL1 INO80H NMP238 TIP49 TIP49A	Up-regulated
P61204	ADP-ribosylation factor 3	ARF3	Up-regulated
P60484	Phosphatidylinositol 3,4,5-trisphosphate 3-phosphatase and dual-specificity protein phosphatase PTEN (EC 3.1.3.16) (EC 3.1.3.48) (EC 3.1.3.67) (Mutated in multiple advanced cancers 1) (Phosphatase and tensin homolog)	PTEN MMAC1 TEP1	Up-regulated
Q8NGA1	Olfactory receptor 1M1 (Olfactory receptor 19-6) (OR19-6) (Olfactory receptor OR19-5)	OR1M1	Up-regulated
P81605	Dermcidin (EC 3.4.-.-) (Preproteolysin) [Cleaved into: Survival-promoting peptide; DCD-1]	DCD AIDD DSEP	Up-regulated
P13473	Lysosome-associated membrane glycoprotein 2 (LAMP-2) (Lysosome-associated membrane protein 2) (CD107 antigen-like family member B) (LGP-96) (CD antigen CD107b)	LAMP2	Up-regulated
P00403	Cytochrome c oxidase subunit 2 (EC 7.1.1.9) (Cytochrome c oxidase polypeptide II)	MT-CO2 COII COX2 COXII MTCO2	Up-regulated
Q9BW60	Elongation of very long chain fatty acids protein 1 (EC 2.3.1.199) (3-keto acyl-CoA synthase ELOVL1) (ELOVL fatty acid elongase 1) (ELOVL FA elongase 1) (Very long chain 3-ketoacyl-CoA synthase 1) (Very long chain 3-oxoacyl-CoA synthase 1)	ELOVL1 SSC1 CGI-88	Up-regulated
Q9UBI6	Guanine nucleotide-binding protein G(I)/G(S)/G(O) subunit gamma-12	GNG12	Up-regulated
Q6P2Q9	Pre-mRNA-processing-splicing factor 8 (220 kDa U5 snRNP-specific protein) (PRP8 homolog) (Splicing factor Prp8) (p220)	PRPF8 PRPC8	Up-regulated

P62851	40S ribosomal protein S25 (Small ribosomal subunit protein eS25)	RPS25	Up-regulated
P46109	Crk-like protein	CRKL	Up-regulated
P49821	NADH dehydrogenase [ubiquinone] flavoprotein 1, mitochondrial (EC 7.1.1.2) (Complex I-51kD) (CI-51kD) (NADH dehydrogenase flavoprotein 1) (NADH-ubiquinone oxidoreductase 51 kDa subunit)	NDUFV1 UQOR1	Up-regulated
O14737	Programmed cell death protein 5 (TF-1 cell apoptosis-related protein 19) (Protein TFAR19)	PDCD5 TFAR19	Up-regulated
Q9NZ01	Very-long-chain enoyl-CoA reductase (EC 1.3.1.93) (Synaptic glycoprotein SC2) (Trans-2,3-enoyl-CoA reductase) (TER)	TECR GPSN2 SC2	Up-regulated
Q96DG6	Carboxymethylenebutenolidase homolog (EC 3.1.-.-)	CMBL	Up-regulated
Q92888	Rho guanine nucleotide exchange factor 1 (115 kDa guanine nucleotide exchange factor) (p115-RhoGEF) (p115RhoGEF) (Sub1.5)	ARHGEF1	Up-regulated
Q9UJU6	Drebrin-like protein (Cervical SH3P7) (Cervical mucin-associated protein) (Drebrin-F) (HPK1-interacting protein of 55 kDa) (HIP-55) (SH3 domain-containing protein 7)	DBNL CMAP SH3P7 PP5423	Up-regulated
P09913	Interferon-induced protein with tetratricopeptide repeats 2 (IFIT-2) (ISG-54 K) (Interferon-induced 54 kDa protein) (IFI-54K) (P54)	IFIT2 CIG-42 G10P2 IFI54 ISG54	Up-regulated
P09110	3-ketoacyl-CoA thiolase, peroxisomal (EC 2.3.1.16) (Acetyl-CoA acyltransferase) (Beta-ketothiolase) (Peroxisomal 3-oxoacyl-CoA thiolase)	ACAA1 ACAA PTHIO	Up-regulated
P13010	X-ray repair cross-complementing protein 5 (EC 3.6.4.-) (86 kDa subunit of Ku antigen) (ATP-dependent DNA helicase 2 subunit 2) (ATP-dependent DNA helicase II 80 kDa subunit) (CTC box-binding factor 85 kDa subunit) (CTC85) (CTCBF) (DNA repair protein XRCC5) (Ku80) (Ku86) (Lupus Ku autoantigen protein p86) (Nuclear factor IV) (Thyroid-lupus autoantigen) (TLAA) (X-ray repair complementing defective repair in Chinese hamster cells 5 (double-strand-break rejoining))	XRCC5 G22P2	Up-regulated

P12955	Xaa-Pro dipeptidase (X-Pro dipeptidase) (EC 3.4.13.9) (Imidodipeptidase) (Peptidase D) (Proline dipeptidase) (Prolidase)	PEPD PRD	Up-regulated
Q96Q42	Alsin (Amyotrophic lateral sclerosis 2 chromosomal region candidate gene 6 protein) (Amyotrophic lateral sclerosis 2 protein)	ALS2 ALS2CR6 KIAA1563	Down-regulated
P78344	Eukaryotic translation initiation factor 4 gamma 2 (eIF-4-gamma 2) (eIF-4G 2) (eIF4G 2) (Death-associated protein 5) (DAP-5) (p97)	EIF4G2 DAP5 OK/SW-cl.75	Down-regulated
Q9UNE7	E3 ubiquitin-protein ligase CHIP (EC 2.3.2.27) (Antigen NY-CO-7) (CLL-associated antigen KW-8) (Carboxy terminus of Hsp70-interacting protein) (RING-type E3 ubiquitin transferase CHIP) (STIP1 homology and U box-containing protein 1)	STUB1 CHIP PP1131	Down-regulated
P55263	Adenosine kinase (AK) (EC 2.7.1.20) (Adenosine 5'-phosphotransferase)	ADK	Down-regulated
Q16204	Coiled-coil domain-containing protein 6 (Papillary thyroid carcinoma-encoded protein) (Protein H4)	CCDC6 D10S170 TST1	Down-regulated
P48047	ATP synthase subunit O, mitochondrial (ATP synthase peripheral stalk subunit OSCP) (Oligomycin sensitivity conferral protein) (OSCP)	ATP5PO ATP5O ATPO	Down-regulated
Q9Y333	U6 snRNA-associated Sm-like protein LSm2 (Protein G7b) (Small nuclear ribonuclear protein D homolog) (snRNP core Sm-like protein Sm-x5)	LSM2 C6orf28 G7B	Down-regulated
Q13561	Dynactin subunit 2 (50 kDa dynein-associated polypeptide) (Dynactin complex 50 kDa subunit) (DCTN-50) (p50 dynamitin)	DCTN2 DCTN50	Down-regulated
Q9P2B4	CTTNBP2 N-terminal-like protein	CTTNBP2NL KIAA1433	Down-regulated
Q15404	Ras suppressor protein 1 (RSP-1) (Rsu-1)	RSU1 RSP1	Down-regulated
O60884	DnaJ homolog subfamily A member 2 (Cell cycle progression restoration gene 3 protein) (Dnj3) (Dj3) (HIRA-interacting protein 4) (Renal carcinoma antigen NY-REN-14)	DNAJA2 CPR3 HIRIP4	Down-regulated
P16035	Metalloproteinase inhibitor 2 (CSC-21K) (Tissue inhibitor of metalloproteinases 2) (TIMP-2)	TIMP2	Down-regulated

Q9NPA8	Transcription and mRNA export factor ENY2 (Enhancer of yellow 2 transcription factor homolog)	ENY2 DC6	Down-regulated
P61927	60S ribosomal protein L37 (G1.16) (Large ribosomal subunit protein eL37)	RPL37	Down-regulated
O95373	Importin-7 (Imp7) (Ran-binding protein 7) (RanBP7)	IPO7 RANBP7	Down-regulated
Q92890	Ubiquitin recognition factor in ER-associated degradation protein 1 (Ubiquitin fusion degradation protein 1) (UB fusion protein 1)	UFD1 UFD1L	Down-regulated
P84090	Enhancer of rudimentary homolog	ERH	Down-regulated
P12270	Nucleoprotein TPR (Megator) (NPC-associated intranuclear protein) (Translocated promoter region protein)	TPR	Down-regulated
O00571	ATP-dependent RNA helicase DDX3X (EC 3.6.4.13) (CAP-Rf) (DEAD box protein 3, X-chromosomal) (DEAD box, X isoform) (DBX) (Helicase-like protein 2) (HLP2)	DDX3X DBX DDX3	Down-regulated
O43795	Unconventional myosin-Ib (MYH-1c) (Myosin I alpha) (MMI-alpha) (MMIa)	MYO1B	Down-regulated
P61313	60S ribosomal protein L15 (Large ribosomal subunit protein eL15)	RPL15 EC45 TCBAP0781	Down-regulated
Q14677	Clathrin interactor 1 (Clathrin-interacting protein localized in the trans-Golgi region) (Clint) (Enthoprotin) (Epsin-4) (Epsin-related protein) (EpsinR)	CLINT1 ENTH EPN4 EPNR KIAA0171	Down-regulated
Q6NYC8	Phostensin (Protein phosphatase 1 F-actin cytoskeleton-targeting subunit) (Protein phosphatase 1 regulatory subunit 18)	PPP1R18 HKMT1098 KIAA1949	Down-regulated
P05198	Eukaryotic translation initiation factor 2 subunit 1 (Eukaryotic translation initiation factor 2 subunit alpha) (eIF-2-alpha) (eIF-2A) (eIF-2alpha)	EIF2S1 EIF2A	Down-regulated
Q13409	Cytoplasmic dynein 1 intermediate chain 2 (Cytoplasmic dynein intermediate chain 2) (Dynein intermediate chain 2, cytosolic) (DH IC-2)	DYNC1I2 DNCI2 DNCIC2	Down-regulated
Q9UHB9	Signal recognition particle subunit SRP68 (SRP68) (Signal recognition particle 68 kDa protein)	SRP68	Down-regulated
Q9UHV9	Prefoldin subunit 2	PFDN2 PFD2 HSPC231	Down-regulated
P53621	Coatomer subunit alpha (Alpha-coat protein) (Alpha-COP) (HEP-COP) (HEPCOP)	COPA	Down-regulated

	[Cleaved into: Xenin (Xenopsin-related peptide); Proxenin]		
P53618	Coatomer subunit beta (Beta-coat protein) (Beta-COP)	COPB1 COPB MSTP026	Down-regulated

Whole list of proteins that were expressed differentially in the comparison between pal_vs_veh with a p_value <0.01 and a FDR <0.1

Supplementary material 2. Full list of differentially expressed proteins in the comparison between tip_vs_veh

Entry	Protein names	Gene names	Protein expression
Q16658	Fascin (55 kDa actin-bundling protein) (Singed-like protein) (p55)	FSCN1 FAN1 HSN SNL	Up-regulated
Q9Y3D6	Mitochondrial fission 1 protein (FIS1 homolog) (hFis1) (Tetratricopeptide repeat protein 11) (TPR repeat protein 11)	FIS1 TTC11 CGI-135	Up-regulated
Q9NQC3	Reticulon-4 (Foocen) (Neurite outgrowth inhibitor) (Nogo protein) (Neuroendocrine-specific protein) (NSP) (Neuroendocrine-specific protein C homolog) (RTN-x) (Reticulon-5)	RTN4 KIAA0886 NOGO My043 SP1507	Up-regulated
O95819	Mitogen-activated protein kinase kinase kinase kinase 4 (EC 2.7.11.1) (HPK/GCK-like kinase HGK) (MAPK/ERK kinase kinase kinase 4) (MEK kinase kinase 4) (MEKKK 4) (Nck-interacting kinase)	MAP4K4 HGK KIAA0687 NIK	Up-regulated
Q4KWH8	1-phosphatidylinositol 4,5-bisphosphate phosphodiesterase eta-1 (EC 3.1.4.11) (Phosphoinositide phospholipase C-eta-1) (Phospholipase C-eta-1) (PLC-eta-1) (Phospholipase C-like protein 3) (PLC-L3)	PLCH1 KIAA1069 PLCL3	Up-regulated
P63167	Dynein light chain 1, cytoplasmic (8 kDa dynein light chain) (DLC8) (Dynein light chain LC8-type 1) (Protein inhibitor of neuronal nitric oxide synthase) (PIN)	DYNLL1 DLC1 DNCL1 DNCLC1 HDLC1	Up-regulated
O75439	Mitochondrial-processing peptidase subunit beta (EC 3.4.24.64) (Beta-MPP) (P-52)	PMPCB MPPB	Up-regulated
P05141	ADP/ATP translocase 2 (ADP,ATP carrier protein 2) (ADP,ATP carrier	SLC25A5 ANT2	Up-regulated

	protein, fibroblast isoform) (Adenine nucleotide translocator 2) (ANT 2) (Solute carrier family 25 member 5) [Cleaved into: ADP/ATP translocase 2, N-terminally processed]		
Q9UHB9	Signal recognition particle subunit SRP68 (SRP68) (Signal recognition particle 68 kDa protein)	SRP68	Up-regulated
O75165	DnaJ homolog subfamily C member 13 (Required for receptor-mediated endocytosis 8) (RME-8)	DNAJC13 KIAA0678 RME8	Up-regulated
O43169	Cytochrome b5 type B (Cytochrome b5 outer mitochondrial membrane isoform)	CYB5B CYB5M OMB5	Up-regulated
P58546	Myotrophin (Protein V-1)	MTPN	Up-regulated
P63096	Guanine nucleotide-binding protein G(i) subunit alpha-1 (Adenylate cyclase-inhibiting G alpha protein)	GNAI1	Up-regulated
Q12904	Aminoacyl tRNA synthase complex-interacting multifunctional protein 1 (Multisynthase complex auxiliary component p43) [Cleaved into: Endothelial monocyte-activating polypeptide 2 (EMAP-2) (Endothelial monocyte-activating polypeptide II) (EMAP-II) (Small inducible cytokine subfamily E member 1)]	AIMP1 EMAP2 SCYE1	Up-regulated
Q13162	Peroxiredoxin-4 (EC 1.11.1.24) (Antioxidant enzyme AOE372) (AOE37-2) (Peroxiredoxin IV) (Prx-IV) (Thioredoxin peroxidase AO372) (Thioredoxin-dependent peroxide reductase A0372) (Thioredoxin-dependent peroxiredoxin 4)	PRDX4	Up-regulated
P21589	5'-nucleotidase (5'-NT) (EC 3.1.3.5) (Ecto-5'-nucleotidase) (CD antigen CD73)	NT5E NT5 NTE	Up-regulated
O75340	Programmed cell death protein 6 (Apoptosis-linked gene 2 protein homolog) (ALG-2)	PDCD6 ALG2	Up-regulated
P09914	Interferon-induced protein with tetratricopeptide repeats 1 (IFIT-1) (Interferon-induced 56 kDa protein) (IFI-56K) (P56)	IFIT1 G10P1 IFI56 IFNAI1 ISG56	Up-regulated

Q14108	Lysosome membrane protein 2 (85 kDa lysosomal membrane sialoglycoprotein) (LGP85) (CD36 antigen-like 2) (Lysosome membrane protein II) (LIMP II) (Scavenger receptor class B member 2) (CD antigen CD36)	SCARB2 CD36L2 LIMP2 LIMPII	Up-regulated
P47755	F-actin-capping protein subunit alpha-2 (CapZ alpha-2)	CAPZA2	Up-regulated
Q6IBS0	Twinfilin-2 (A6-related protein) (hA6RP) (Protein tyrosine kinase 9-like) (Twinfilin-1-like protein)	TWF2 PTK9L MSTP011	Up-regulated
P14174	Macrophage migration inhibitory factor (MIF) (EC 5.3.2.1) (Glycosylation-inhibiting factor) (GIF) (L-dopachrome isomerase) (L-dopachrome tautomerase) (EC 5.3.3.12) (Phenylpyruvate tautomerase)	MIF GLIF MMIF	Up-regulated
P60903	Protein S100-A10 (Calpactin I light chain) (Calpactin-1 light chain) (Cellular ligand of annexin II) (S100 calcium-binding protein A10) (p10 protein) (p11)	S100A10 ANX2LG CAL1L CLP11	Up-regulated
P06703	Protein S100-A6 (Calcyclin) (Growth factor-inducible protein 2A9) (MLN 4) (Prolactin receptor-associated protein) (PRA) (S100 calcium-binding protein A6)	S100A6 CACY	Up-regulated
P06744	Glucose-6-phosphate isomerase (GPI) (EC 5.3.1.9) (Autocrine motility factor) (AMF) (Neuroleukin) (NLK) (Phosphoglucose isomerase) (PGI) (Phosphohexose isomerase) (PHI) (Sperm antigen 36) (SA-36)	GPI	Up-regulated
P52594	Arf-GAP domain and FG repeat-containing protein 1 (HIV-1 Rev-binding protein) (Nucleoporin-like protein RIP) (Rev-interacting protein) (Rev/Rex activation domain-binding protein)	AGFG1 HRB RAB RIP	Up-regulated
Q03518	Antigen peptide transporter 1 (APT1) (ATP-binding cassette sub-family B member 2) (Peptide supply factor 1) (Peptide transporter PSF1) (PSF-1) (Peptide transporter TAP1) (Peptide	TAP1 ABCB2 PSF1 RING4 Y3	Up-regulated

	transporter involved in antigen processing 1) (Really interesting new gene 4 protein)		
P07355	Annexin A2 (Annexin II) (Annexin-2) (Calpactin I heavy chain) (Calpactin-1 heavy chain) (Chromobindin-8) (Lipocortin II) (Placental anticoagulant protein IV) (PAP-IV) (Protein I) (p36)	ANXA2 ANX2 ANX2L4 CAL1H LPC2D	Up-regulated
Q92882	Osteoclast-stimulating factor 1	OSTF1	Up-regulated
P62851	40S ribosomal protein S25 (Small ribosomal subunit protein eS25)	RPS25	Up-regulated
O60502	Protein O-GlcNAcase (OGA) (EC 3.2.1.169) (Beta-N-acetylglucosaminidase) (Beta-N-acetylhexosaminidase) (Beta-hexosaminidase) (Meningioma-expressed antigen 5) (N-acetyl-beta-D-glucosaminidase) (N-acetyl-beta-glucosaminidase) (Nuclear cytoplasmic O-GlcNAcase and acetyltransferase) (NCOAT)	OGA HEXC KIAA0679 MEA5 MGEA5	Up-regulated
Q9HAY6	Beta,beta-carotene 15,15'-dioxygenase (EC 1.13.11.63) (Beta-carotene dioxygenase 1) (Beta-carotene oxygenase 1)	BCO1 BCDO BCDO1 BCMO1	Up-regulated
P60484	Phosphatidylinositol 3,4,5-trisphosphate 3-phosphatase and dual-specificity protein phosphatase PTEN (EC 3.1.3.16) (EC 3.1.3.48) (EC 3.1.3.67) (Mutated in multiple advanced cancers 1) (Phosphatase and tensin homolog)	PTEN MMAC1 TEP1	Up-regulated
Q96TA1	Protein Niban 2 (Meg-3) (Melanoma invasion by ERK) (MINERVA) (Niban-like protein 1) (Protein FAM129B)	NIBAN2 C9orf88 FAM129B	Up-regulated
Q92888	Rho guanine nucleotide exchange factor 1 (115 kDa guanine nucleotide exchange factor) (p115-RhoGEF) (p115RhoGEF) (Sub1.5)	ARHGEF1	Up-regulated
P84085	ADP-ribosylation factor 5	ARF5	Up-regulated
P04264	Keratin, type II cytoskeletal 1 (67 kDa cytokeratin) (Cytokeratin-1) (CK-1)	KRT1 KRTA	Up-regulated

	(Hair alpha protein) (Keratin-1) (K1) (Type-II keratin Kb1)		
P49902	Cytosolic purine 5'-nucleotidase (EC 3.1.3.5) (Cytosolic 5'-nucleotidase II)	NT5C2 NT5B NT5CP PNT5	Up-regulated
Q9Y646	Carboxypeptidase Q (EC 3.4.17.-) (Lysosomal dipeptidase) (Plasma glutamate carboxypeptidase)	CPQ LCH1 PGCP	Up-regulated
P29692	Elongation factor 1-delta (EF-1-delta) (Antigen NY-CO-4)	EEF1D EF1D	Up-regulated
Q8IWB7	WD repeat and FYVE domain-containing protein 1 (FYVE domain-containing protein localized to endosomes 1) (FENS-1) (Phosphoinositide-binding protein 1) (WD40- and FYVE domain-containing protein 1) (Zinc finger FYVE domain-containing protein 17)	WDFY1 FENS1 KIAA1435 WDF1 ZFYVE17	Up-regulated
Q96DG6	Carboxymethylenebutenolidase homolog (EC 3.1.-.-)	CMBL	Up-regulated
Q5QNW6	Histone H2B type 2-F (H2B-clustered histone 18)	H2BC18 HIST2H2BF	Up-regulated
Q7L014	Probable ATP-dependent RNA helicase DDX46 (EC 3.6.4.13) (DEAD box protein 46) (PRP5 homolog)	DDX46 KIAA0801	Up-regulated
Q9BW60	Elongation of very long chain fatty acids protein 1 (EC 2.3.1.199) (3-keto acyl-CoA synthase ELOVL1) (ELOVL fatty acid elongase 1) (ELOVL FA elongase 1) (Very long chain 3-ketoacyl-CoA synthase 1) (Very long chain 3-oxoacyl-CoA synthase 1)	ELOVL1 SSC1 CGI-88	Up-regulated
O14879	Interferon-induced protein with tetratricopeptide repeats 3 (IFIT-3) (CIG49) (ISG-60) (Interferon-induced 60 kDa protein) (IFI-60K) (Interferon-induced protein with tetratricopeptide repeats 4) (IFIT-4) (Retinoic acid-induced gene G protein) (P60) (RIG-G)	IFIT3 CIG-49 IFI60 IFIT4 ISG60	Up-regulated
P00403	Cytochrome c oxidase subunit 2 (EC 7.1.1.9) (Cytochrome c oxidase polypeptide II)	MT-CO2 COII COX2 COXII MTCO2	Up-regulated

P19367	Hexokinase-1 (EC 2.7.1.1) (Brain form hexokinase) (Hexokinase type I) (HK I) (Hexokinase-A)	HK1	Up-regulated
P09110	3-ketoacyl-CoA thiolase, peroxisomal (EC 2.3.1.16) (Acetyl-CoA acyltransferase) (Beta-ketothiolase) (Peroxisomal 3-oxoacyl-CoA thiolase)	ACAA1 ACAA PTHIO	Up-regulated
O95497	Pantetheinase (EC 3.5.1.92) (Pantetheine hydrolase) (Tiff66) (Vascular non-inflammatory molecule 1) (Vanin-1)	VNN1	Up-regulated
Q9UBI6	Guanine nucleotide-binding protein G(I)/G(S)/G(O) subunit gamma-12	GNG12	Up-regulated
P12235	ADP/ATP translocase 1 (ADP,ATP carrier protein 1) (ADP,ATP carrier protein, heart/skeletal muscle isoform T1) (Adenine nucleotide translocator 1) (ANT 1) (Solute carrier family 25 member 4)	SLC25A4 ANT1	Up-regulated
P62805	Histone H4	H4C1 H4/A H4FA HIST1H4A; H4C2 H4/I H4FI HIST1H4B; H4C3 H4/G H4FG HIST1H4C; H4C4 H4/B H4FB HIST1H4D; H4C5 H4/J H4FJ HIST1H4E; H4C6 H4/C H4FC HIST1H4F; H4C8 H4/H H4FH HIST1H4H; H4C9 H4/M H4FM HIST1H4I; H4C11 H4/E H4FE HIST1H4J; H4C12 H4/D H4FD HIST1H4K; H4C13 H4/K H4FK HIST1H4L; H4C14 H4/N H4F2 H4FN HIST2H4 HIST2H4A; H4C15 H4/O H4FO	Up-regulated

		HIST2H4B; H4-16 HIST4H4	
O95573	Long-chain-fatty-acid--CoA ligase 3 (EC 6.2.1.3) (Arachidonate--CoA ligase) (EC 6.2.1.15) (Long-chain acyl-CoA synthetase 3) (LACS 3)	ACSL3 ACS3 FACL3 LACS3	Up-regulated
O14737	Programmed cell death protein 5 (TF-1 cell apoptosis-related protein 19) (Protein TFAR19)	PDCD5 TFAR19	Up-regulated
P13010	X-ray repair cross-complementing protein 5 (EC 3.6.4.-) (86 kDa subunit of Ku antigen) (ATP-dependent DNA helicase 2 subunit 2) (ATP-dependent DNA helicase II 80 kDa subunit) (CTC box-binding factor 85 kDa subunit) (CTC85) (CTCBF) (DNA repair protein XRCC5) (Ku80) (Ku86) (Lupus Ku autoantigen protein p86) (Nuclear factor IV) (Thyroid-lupus autoantigen) (TLAA) (X-ray repair complementing defective repair in Chinese hamster cells 5 (double-strand-break rejoining))	XRCC5 G22P2	Up-regulated
P09913	Interferon-induced protein with tetratricopeptide repeats 2 (IFIT-2) (ISG-54 K) (Interferon-induced 54 kDa protein) (IFI-54K) (P54)	IFIT2 CIG-42 G10P2 IFI54 ISG54	Up-regulated
Q96Q42	Alsin (Amyotrophic lateral sclerosis 2 chromosomal region candidate gene 6 protein) (Amyotrophic lateral sclerosis 2 protein)	ALS2 ALS2CR6 KIAA1563	Down-regulated
P53618	Coatomer subunit beta (Beta-coat protein) (Beta-COP)	COPB1 COPB MSTP026	Down-regulated
O43294	Transforming growth factor beta-1-induced transcript 1 protein (Androgen receptor coactivator 55 kDa protein) (Androgen receptor-associated protein of 55 kDa) (Hydrogen peroxide-inducible clone 5 protein) (Hic-5)	TGFB1I1 ARA55	Down-regulated
Q9NX63	MICOS complex subunit MIC19 (Coiled-coil-helix-coiled-coil-helix domain-containing protein 3)	CHCHD3 MIC19 MINOS3	Down-regulated
O43795	Unconventional myosin-Ib (MYH-1c) (Myosin I alpha) (MMI-alpha) (MMIa)	MYO1B	Down-regulated

Q9NP79	Vacuolar protein sorting-associated protein VTA1 homolog (Dopamine-responsive gene 1 protein) (DRG-1) (LYST-interacting protein 5) (LIP5) (SKD1-binding protein 1) (SBP1)	VTA1 C6orf55 HSPC228 My012	Down-regulated
Q9UNE7	E3 ubiquitin-protein ligase CHIP (EC 2.3.2.27) (Antigen NY-CO-7) (CLL-associated antigen KW-8) (Carboxy terminus of Hsp70-interacting protein) (RING-type E3 ubiquitin transferase CHIP) (STIP1 homology and U box-containing protein 1)	STUB1 CHIP PP1131	Down-regulated
Q9P2B4	CTTNBP2 N-terminal-like protein	CTTNBP2NL KIAA1433	Down-regulated
P46459	Vesicle-fusing ATPase (EC 3.6.4.6) (N-ethylmaleimide-sensitive fusion protein) (NEM-sensitive fusion protein) (Vesicular-fusion protein NSF)	NSF	Down-regulated
P21399	Cytoplasmic aconitate hydratase (Aconitase) (EC 4.2.1.3) (Citrate hydro-lyase) (Ferritin repressor protein) (Iron regulatory protein 1) (IRP1) (Iron-responsive element-binding protein 1) (IRE-BP 1)	ACO1 IREB1	Down-regulated
Q08211	ATP-dependent RNA helicase A (EC 3.6.4.13) (DEAH box protein 9) (DExH-box helicase 9) (Leukophysin) (LKP) (Nuclear DNA helicase II) (NDH II) (RNA helicase A)	DHX9 DDX9 LKP NDH2	Down-regulated
Q1KMD3	Heterogeneous nuclear ribonucleoprotein U-like protein 2 (Scaffold-attachment factor A2) (SAF-A2)	HNRNPUL2 HNRPUL2	Down-regulated
P54578	Ubiquitin carboxyl-terminal hydrolase 14 (EC 3.4.19.12) (Deubiquitinating enzyme 14) (Ubiquitin thioesterase 14) (Ubiquitin-specific-processing protease 14)	USP14 TGT	Down-regulated
Q04637	Eukaryotic translation initiation factor 4 gamma 1 (eIF-4-gamma 1) (eIF-4G 1) (eIF-4G1) (p220)	EIF4G1 EIF4F EIF4G EIF4GI	Down-regulated
Q15165	Serum paraoxonase/arylesterase 2 (PON 2) (EC 3.1.1.2) (EC 3.1.1.81) (Aromatic esterase 2) (A-esterase 2) (Serum aryldialkylphosphatase 2)	PON2	Down-regulated

P43487	Ran-specific GTPase-activating protein (Ran-binding protein 1) (RanBP1)	RANBP1	Down-regulated
P22061	Protein-L-isoaspartate(D-aspartate) O-methyltransferase (PIMT) (EC 2.1.1.77) (L-isoaspartyl protein carboxyl methyltransferase) (Protein L-isoaspartyl/D-aspartyl methyltransferase) (Protein-beta-aspartate methyltransferase)	PCMT1	Down-regulated
P16035	Metalloproteinase inhibitor 2 (CSC-21K) (Tissue inhibitor of metalloproteinases 2) (TIMP-2)	TIMP2	Down-regulated
O60884	DnaJ homolog subfamily A member 2 (Cell cycle progression restoration gene 3 protein) (Dnj3) (Dj3) (HIRA-interacting protein 4) (Renal carcinoma antigen NY-REN-14)	DNAJA2 CPR3 HIRIP4	Down-regulated
Q9Y333	U6 snRNA-associated Sm-like protein LSm2 (Protein G7b) (Small nuclear ribonuclear protein D homolog) (snRNP core Sm-like protein Sm-x5)	LSM2 C6orf28 G7B	Down-regulated
P55263	Adenosine kinase (AK) (EC 2.7.1.20) (Adenosine 5'-phosphotransferase)	ADK	Down-regulated
Q12792	Twinfilin-1 (Protein A6) (Protein tyrosine kinase 9)	TWF1 PTK9	Down-regulated
P83731	60S ribosomal protein L24 (60S ribosomal protein L30) (Large ribosomal subunit protein eL24)	RPL24	Down-regulated
O00571	ATP-dependent RNA helicase DDX3X (EC 3.6.4.13) (CAP-Rf) (DEAD box protein 3, X-chromosomal) (DEAD box, X isoform) (DBX) (Helicase-like protein 2) (HLP2)	DDX3X DBX DDX3	Down-regulated
P43243	Matrin-3	MATR3 KIAA0723	Down-regulated
O00629	Importin subunit alpha-3 (Importin alpha Q1) (Qip1) (Karyopherin subunit alpha-4)	KPNA4 QIP1	Down-regulated
Q9NTK5	Obg-like ATPase 1 (DNA damage-regulated overexpressed in cancer 45) (DOC45) (GTP-binding protein 9)	OLA1 GTPBP9 PRO2455 PTD004	Down-regulated
Q02809	Procollagen-lysine,2-oxoglutarate 5-dioxygenase 1 (EC 1.14.11.4) (Lysyl hydroxylase 1) (LH1)	PLOD1 LLH PLOD	Down-regulated

Q9NY33	Dipeptidyl peptidase 3 (EC 3.4.14.4) (Dipeptidyl aminopeptidase III) (Dipeptidyl arylamidase III) (Dipeptidyl peptidase III) (DPP III) (Enkephalinase B)	DPP3	Down-regulated
Q14194	Dihydropyrimidinase-related protein 1 (DRP-1) (Collapsin response mediator protein 1) (CRMP-1) (Inactive dihydropyrimidinase) (Unc-33-like phosphoprotein 3) (ULIP-3)	CRMP1 DPYSL1 ULIP3	Down-regulated
Q92896	Golgi apparatus protein 1 (CFR-1) (Cysteine-rich fibroblast growth factor receptor) (E-selectin ligand 1) (ESL-1) (Golgi sialoglycoprotein MG-160)	GLG1 CFR1 ESL1 MG160	Down-regulated
P61313	60S ribosomal protein L15 (Large ribosomal subunit protein eL15)	RPL15 EC45 TCBAP0781	Down-regulated
Q9H0U4	Ras-related protein Rab-1B	RAB1B	Down-regulated
Q9NYF8	Bcl-2-associated transcription factor 1 (Btf) (BCLAF1 and THRAP3 family member 1)	BCLAF1 BTF KIAA0164	Down-regulated
Q9UNM6	26S proteasome non-ATPase regulatory subunit 13 (26S proteasome regulatory subunit RPN9) (26S proteasome regulatory subunit S11) (26S proteasome regulatory subunit p40.5)	PSMD13	Down-regulated
Q5JPE7	Nodal modulator 2 (pM5 protein 2)	NOMO2	Down-regulated
Q92890	Ubiquitin recognition factor in ER-associated degradation protein 1 (Ubiquitin fusion degradation protein 1) (UB fusion protein 1)	UFD1 UFD1L	Down-regulated
Q9Y2S6	Translation machinery-associated protein 7 (Coiled-coil domain-containing protein 72)	TMA7 CCDC72 HSPC016 HSPC330	Down-regulated
Q13510	Acid ceramidase (AC) (ACDase) (Acid CDase) (EC 3.5.1.23) (Acylsphingosine deacylase) (N-acylethanolamine hydrolase ASAH1) (EC 3.5.1.-) (N-acylsphingosine amidohydrolase) (Putative 32 kDa heart protein) (PHP32) [Cleaved into: Acid ceramidase subunit alpha; Acid ceramidase subunit beta]	ASAH1 ASAH HSD-33 HSD33	Down-regulated

P14927	Cytochrome b-c1 complex subunit 7 (Complex III subunit 7) (Complex III subunit VII) (QP-C) (Ubiquinol-cytochrome c reductase complex 14 kDa protein)	UQCRB UQBP	Down-regulated
P50570	Dynamin-2 (EC 3.6.5.5)	DNM2 DYN2	Down-regulated
Q7Z6Z7	E3 ubiquitin-protein ligase HUWE1 (EC 2.3.2.26) (ARF-binding protein 1) (ARF-BP1) (HECT, UBA and WWE domain-containing protein 1) (HECT-type E3 ubiquitin transferase HUWE1) (Homologous to E6AP carboxyl terminus homologous protein 9) (HectH9) (Large structure of UREB1) (LASU1) (Mcl-1 ubiquitin ligase E3) (Mule) (Upstream regulatory element-binding protein 1) (URE-B1) (URE-binding protein 1)	HUWE1 KIAA0312 KIAA1578 UREB1 HSPC272	Down-regulated
Q92598	Heat shock protein 105 kDa (Antigen NY-CO-25) (Heat shock 110 kDa protein)	HSPH1 HSP105 HSP110 KIAA0201	Down-regulated
O00244	Copper transport protein ATOX1 (Metal transport protein ATX1)	ATOX1 HAH1	Down-regulated
O00231	26S proteasome non-ATPase regulatory subunit 11 (26S proteasome regulatory subunit RPN6) (26S proteasome regulatory subunit S9) (26S proteasome regulatory subunit p44.5)	PSMD11	Down-regulated
Q8WUP2	Filamin-binding LIM protein 1 (FBLP-1) (Migfilin) (Mitogen-inducible 2-interacting protein) (MIG2-interacting protein)	FBLIM1 FBLP1	Down-regulated
P25786	Proteasome subunit alpha type-1 (EC 3.4.25.1) (30 kDa prosomal protein) (PROS-30) (Macropain subunit C2) (Multicatalytic endopeptidase complex subunit C2) (Proteasome component C2) (Proteasome nu chain)	PSMA1 HC2 NU PROS30 PSC2	Down-regulated
P05121	Plasminogen activator inhibitor 1 (PAI) (PAI-1) (Endothelial plasminogen activator inhibitor) (Serpin E1)	SERPINE1 PAI1 PLANH1	Down-regulated
P52597	Heterogeneous nuclear ribonucleoprotein F (hnRNP F)	HNRNPF HNRPF	Down-regulated

	(Nucleolin-like protein mcs94-1) [Cleaved into: Heterogeneous nuclear ribonucleoprotein F, N-terminally processed]		
Q9UBR2	Cathepsin Z (EC 3.4.18.1) (Cathepsin P) (Cathepsin X)	CTSZ	Down-regulated
O43615	Mitochondrial import inner membrane translocase subunit TIM44	TIMM44 MIMT44 TIM44	Down-regulated
P60468	Protein transport protein Sec61 subunit beta	SEC61B	Down-regulated
P61513	60S ribosomal protein L37a (Large ribosomal subunit protein eL43)	RPL37A	Down-regulated
P10253	Lysosomal alpha-glucosidase (EC 3.2.1.20) (Acid maltase) (Aglucosidase alfa) [Cleaved into: 76 kDa lysosomal alpha-glucosidase; 70 kDa lysosomal alpha-glucosidase]	GAA	Down-regulated
P42766	60S ribosomal protein L35 (Large ribosomal subunit protein uL29)	RPL35	Down-regulated
P12270	Nucleoprotein TPR (Megator) (NPC-associated intranuclear protein) (Translocated promoter region protein)	TPR	Down-regulated
Q15404	Ras suppressor protein 1 (RSP-1) (Rsu-1)	RSU1 RSP1	Down-regulated
P05198	Eukaryotic translation initiation factor 2 subunit 1 (Eukaryotic translation initiation factor 2 subunit alpha) (eIF-2-alpha) (eIF-2A) (eIF-2alpha)	EIF2S1 EIF2A	Down-regulated
P48047	ATP synthase subunit O, mitochondrial (ATP synthase peripheral stalk subunit OSCP) (Oligomycin sensitivity conferral protein) (OSCP)	ATP5PO ATP5O ATPO	Down-regulated
Q15121	Astrocytic phosphoprotein PEA-15 (15 kDa phosphoprotein enriched in astrocytes) (Phosphoprotein enriched in diabetes) (PED)	PEA15	Down-regulated
Q14677	Clathrin interactor 1 (Clathrin-interacting protein localized in the trans-Golgi region) (Clint) (Enthoprotin) (Epsin-4) (Epsin-related protein) (EpsinR)	CLINT1 ENTH EPN4 EPNR KIAA0171	Down-regulated
Q99426	Tubulin-folding cofactor B (Cytoskeleton-associated protein 1) (Cytoskeleton-associated protein	TBCB CG22 CKAP1	Down-regulated

	CKAPI) (Tubulin-specific chaperone B)		
Q9UHB6	LIM domain and actin-binding protein 1 (Epithelial protein lost in neoplasm)	LIMA1 EPLIN SREBP3 PP624	Down-regulated
Q562R1	Beta-actin-like protein 2 (Kappa-actin)	ACTBL2	Down-regulated
P83916	Chromobox protein homolog 1 (HP1Hsbeta) (Heterochromatin protein 1 homolog beta) (HP1 beta) (Heterochromatin protein p25) (M31) (Modifier 1 protein) (p25beta)	CBX1 CBX	Down-regulated
P52943	Cysteine-rich protein 2 (CRP-2) (Protein ESP1)	CRIP2 CRP2	Down-regulated
Q14192	Four and a half LIM domains protein 2 (FHL-2) (LIM domain protein DRAL) (Skeletal muscle LIM-protein 3) (SLIM-3)	FHL2 DRAL SLIM3	Down-regulated
Q9UKY7	Protein CDV3 homolog	CDV3 H41	Down-regulated
Q13409	Cytoplasmic dynein 1 intermediate chain 2 (Cytoplasmic dynein intermediate chain 2) (Dynein intermediate chain 2, cytosolic) (DH IC-2)	DYNC1I2 DNCI2 DNCIC2	Down-regulated
P26599	Polypyrimidine tract-binding protein 1 (PTB) (57 kDa RNA-binding protein PPTB-1) (Heterogeneous nuclear ribonucleoprotein I) (hnRNP I)	PTBP1 PTB	Down-regulated
O60749	Sorting nexin-2 (Transformation-related gene 9 protein) (TRG-9)	SNX2 TRG9	Down-regulated

Whole list of proteins that were expressed differentially in the comparison between tip_vs_veh with a p_value <0.01 and an FDR <0.1

Supplementary material 3. Full list of differentially expressed proteins in the comparison between tip_vs_pal

Entry	Protein names	Gene names	Protein expression
O94905	Erlin-2 (Endoplasmic reticulum lipid raft-associated protein 2) (Stomatin-prohibitin-flotillin-HflC/K domain-containing protein 2) (SPFH domain-containing protein 2)	ERLIN2 C8orf2 SPFH2 UNQ2441/PRO5003/PRO9924	Up-regulated

P62829	60S ribosomal protein L23 (60S ribosomal protein L17) (Large ribosomal subunit protein uL14)	RPL23	Up-regulated
Q6NYC8	Phostensin (Protein phosphatase 1 F-actin cytoskeleton-targeting subunit) (Protein phosphatase 1 regulatory subunit 18)	PPP1R18 HKMT1098 KIAA1949	Up-regulated
O75340	Programmed cell death protein 6 (Apoptosis-linked gene 2 protein homolog) (ALG-2)	PDCD6 ALG2	Up-regulated
P20290	Transcription factor BTF3 (Nascent polypeptide-associated complex subunit beta) (NAC-beta) (RNA polymerase B transcription factor 3)	BTF3 NACB OK/SW-cl.8	Up-regulated
Q9UK76	Jupiter microtubule associated homolog 1 (Androgen-regulated protein 2) (Hematological and neurological expressed 1 protein) [Cleaved into: Jupiter microtubule associated homolog 1, N-terminally processed]	JPT1 ARM2 HN1	Up-regulated
P53992	Protein transport protein Sec24C (SEC24-related protein C)	SEC24C KIAA0079	Up-regulated
P07305	Histone H1.0 (Histone H1') (Histone H1(0)) [Cleaved into: Histone H1.0, N-terminally processed]	H1-0 H1F0 H1FV	Up-regulated
Q92882	Osteoclast-stimulating factor 1	OSTF1	Up-regulated
P28062	Proteasome subunit beta type-8 (EC 3.4.25.1) (Low molecular mass protein 7) (Macropain subunit C13) (Multicatalytic endopeptidase complex subunit C13) (Proteasome component C13) (Proteasome subunit beta-5i)	PSMB8 LMP7 PSMB5i RING10 Y2	Up-regulated

	(Really interesting new gene 10 protein)		
P27708	CAD protein [Includes: Glutamine-dependent carbamoyl-phosphate synthase (EC 6.3.5.5); Aspartate carbamoyltransferase (EC 2.1.3.2); Dihydroorotase (EC 3.5.2.3)]	CAD	Up-regulated
Q13561	Dynactin subunit 2 (50 kDa dynein-associated polypeptide) (Dynactin complex 50 kDa subunit) (DCTN-50) (p50 dynamitin)	DCTN2 DCTN50	Up-regulated
Q9UHB9	Signal recognition particle subunit SRP68 (SRP68) (Signal recognition particle 68 kDa protein)	SRP68	Up-regulated
Q99729	Heterogeneous nuclear ribonucleoprotein A/B (hnRNP A/B) (APOBEC1-binding protein 1) (ABBP-1)	HNRNPAB ABBP1 HNRPAB	Up-regulated
Q16204	Coiled-coil domain-containing protein 6 (Papillary thyroid carcinoma-encoded protein) (Protein H4)	CCDC6 D10S170 TST1	Up-regulated
P78344	Eukaryotic translation initiation factor 4 gamma 2 (eIF-4-gamma 2) (eIF-4G 2) (eIF4G 2) (Death-associated protein 5) (DAP-5) (p97)	EIF4G2 DAP5 OK/SW-cl.75	Up-regulated
Q02750	Dual specificity mitogen-activated protein kinase kinase 1 (MAP kinase kinase 1) (MAPKK 1) (MKK1) (EC 2.7.12.2) (ERK activator kinase 1) (MAPK/ERK kinase 1) (MEK 1)	MAP2K1 MEK1 PRKMK1	Up-regulated
P12955	Xaa-Pro dipeptidase (X-Pro dipeptidase) (EC 3.4.13.9) (Imidodipeptidase) (Peptidase D) (Proline dipeptidase) (Prolidase)	PEPD PRD	Down-regulated

Q9NX63	MICOS complex subunit MIC19 (Coiled-coil-helix-coiled-coil-helix domain-containing protein 3)	CHCHD3 MIC19 MINOS3	Down-regulated
Q15165	Serum paraoxonase/arylesterase 2 (PON 2) (EC 3.1.1.2) (EC 3.1.1.81) (Aromatic esterase 2) (A-esterase 2) (Serum aryldialkylphosphatase 2)	PON2	Down-regulated
Q9UJU6	Drebrin-like protein (Cervical SH3P7) (Cervical mucin-associated protein) (Drebrin-F) (HPK1-interacting protein of 55 kDa) (HIP-55) (SH3 domain-containing protein 7)	DBNL CMAP SH3P7 PP5423	Down-regulated
O43294	Transforming growth factor beta-1-induced transcript 1 protein (Androgen receptor coactivator 55 kDa protein) (Androgen receptor-associated protein of 55 kDa) (Hydrogen peroxide-inducible clone 5 protein) (Hic-5)	TGFB1I1 ARA55	Down-regulated
P21399	Cytoplasmic aconitate hydratase (Aconitase) (EC 4.2.1.3) (Citrate hydro-lyase) (Ferritin repressor protein) (Iron regulatory protein 1) (IRP1) (Iron-responsive element-binding protein 1) (IRE-BP 1)	ACO1 IREB1	Down-regulated
Q9NZ01	Very-long-chain enoyl-CoA reductase (EC 1.3.1.93) (Synaptic glycoprotein SC2) (Trans-2,3-enoyl-CoA reductase) (TER)	TECR GPSN2 SC2	Down-regulated
P53618	Coatomer subunit beta (Beta-coat protein) (Beta-COP)	COPB1 COPB MSTP026	Down-regulated
O43615	Mitochondrial import inner membrane translocase subunit TIM44	TIMM44 MIMT44 TIM44	Down-regulated
Q12792	Twinfilin-1 (Protein A6) (Protein tyrosine kinase 9)	TWF1 PTK9	Down-regulated

P14927	Cytochrome b-c1 complex subunit 7 (Complex III subunit 7) (Complex III subunit VII) (QP-C) (Ubiquinol-cytochrome c reductase complex 14 kDa protein)	UQCRB UQBP	Down-regulated
Q9NY33	Dipeptidyl peptidase 3 (EC 3.4.14.4) (Dipeptidyl aminopeptidase III) (Dipeptidyl arylamidase III) (Dipeptidyl peptidase III) (DPP III) (Enkephalinase B)	DPP3	Down-regulated
P54578	Ubiquitin carboxyl-terminal hydrolase 14 (EC 3.4.19.12) (Deubiquitinating enzyme 14) (Ubiquitin thioesterase 14) (Ubiquitin-specific-processing protease 14)	USP14 TGT	Down-regulated
Q9NTK5	Obg-like ATPase 1 (DNA damage-regulated overexpressed in cancer 45) (DOC45) (GTP-binding protein 9)	OLA1 GTPBP9 PRO2455 PTD004	Down-regulated
Q9H0U4	Ras-related protein Rab-1B	RAB1B	Down-regulated
P42167	Lamina-associated polypeptide 2, isoforms beta/gamma (Thymopoietin, isoforms beta/gamma) (TP beta/gamma) (Thymopoietin-related peptide isoforms beta/gamma) (TPRP isoforms beta/gamma) [Cleaved into: Thymopoietin (TP) (Splenin); Thymopentin (TP5)]	TMPO LAP2	Down-regulated
P10253	Lysosomal alpha-glucosidase (EC 3.2.1.20) (Acid maltase) (Aglucosidase alfa) [Cleaved into: 76 kDa lysosomal alpha-glucosidase; 70 kDa lysosomal alpha-glucosidase]	GAA	Down-regulated
O95336	6-phosphogluconolactonase (6PGL) (EC 3.1.1.31)	PGLS	Down-regulated

P52597	Heterogeneous nuclear ribonucleoprotein F (hnRNP F) (Nucleolin-like protein mcs94-1) [Cleaved into: Heterogeneous nuclear ribonucleoprotein F, N-terminally processed]	HNRNPF HNRPF	Down-regulated
O76094	Signal recognition particle subunit SRP72 (SRP72) (Signal recognition particle 72 kDa protein)	SRP72	Down-regulated
Q5JPE7	Nodal modulator 2 (pM5 protein 2)	NOMO2	Down-regulated
P83916	Chromobox protein homolog 1 (HP1Hsbeta) (Heterochromatin protein 1 homolog beta) (HP1 beta) (Heterochromatin protein p25) (M31) (Modifier 1 protein) (p25beta)	CBX1 CBX	Down-regulated
O00231	26S proteasome non-ATPase regulatory subunit 11 (26S proteasome regulatory subunit RPN6) (26S proteasome regulatory subunit S9) (26S proteasome regulatory subunit p44.5)	PSMD11	Down-regulated
Q15046	Lysine--tRNA ligase (EC 2.7.7.-) (EC 6.1.1.6) (Lysyl-tRNA synthetase) (LysRS)	KARS1 KARS KIAA0070	Down-regulated
O43795	Unconventional myosin-Ib (MYH-1c) (Myosin I alpha) (MMI-alpha) (MMIa)	MYO1B	Down-regulated
Q9BZL1	Ubiquitin-like protein 5	UBL5	Down-regulated
Q16775	Hydroxyacylglutathione hydrolase, mitochondrial (EC 3.1.2.6) (Glyoxalase II) (Glx II)	HAGH GLO2 HAGH1	Down-regulated
P52943	Cysteine-rich protein 2 (CRP-2) (Protein ESP1)	CRIP2 CRP2	Down-regulated

Whole list of proteins that were expressed differentially in the comparison between tip_vs_pal with a p_value <0.01 and an FDR <0.1

Supplementary material 4. Full list of proteins that were unique in the comparison of pal_vs_veh

Entry	Protein names	Gene names	Protein expression
P31949	Protein S100-A11 (Calgizzarin) (Metastatic lymph node gene 70 protein) (MLN 70) (Protein S100-C) (S100 calcium-binding protein A11) [Cleaved into: Protein S100-A11, N-terminally processed]	S100A11 MLN70 S100C	Up-regulated
Q9P2R7	Succinate--CoA ligase [ADP-forming] subunit beta, mitochondrial (EC 6.2.1.5) (ATP-specific succinyl-CoA synthetase subunit beta) (A-SCS) (Succinyl-CoA synthetase beta-A chain) (SCS-betaA)	SUCLA2	Up-regulated
Q9Y265	RuvB-like 1 (EC 3.6.4.12) (49 kDa TATA box-binding protein-interacting protein) (49 kDa TBP-interacting protein) (54 kDa erythrocyte cytosolic protein) (ECP-54) (INO80 complex subunit H) (Nuclear matrix protein 238) (NMP 238) (Pontin 52) (TIP49a) (TIP60-associated protein 54-alpha) (TAP54-alpha)	RUVBL1 INO80H NMP238 TIP49 TIP49A	Up-regulated
P61204	ADP-ribosylation factor 3	ARF3	Up-regulated
Q8NGA1	Olfactory receptor 1M1 (Olfactory receptor 19-6) (OR19-6) (Olfactory receptor OR19-5)	OR1M1	Up-regulated
P81605	Dermcidin (EC 3.4.-.-) (Preproteolysin) [Cleaved into: Survival-promoting peptide; DCD-1]	DCD AIDD DSEP	Up-regulated
P13473	Lysosome-associated membrane glycoprotein 2 (LAMP-2) (Lysosome-associated membrane protein 2) (CD107 antigen-like family member B) (LGP-96) (CD antigen CD107b)	LAMP2	Up-regulated
Q6P2Q9	Pre-mRNA-processing-splicing factor 8 (220 kDa U5 snRNP-specific protein) (PRP8 homolog) (Splicing factor Prp8) (p220)	PRPF8 PRPC8	Up-regulated
P46109	Crk-like protein	CRKL	Up-regulated
P49821	NADH dehydrogenase [ubiquinone] flavoprotein 1, mitochondrial (EC 7.1.1.2) (Complex I-51kD) (CI-51kD) (NADH dehydrogenase flavoprotein 1) (NADH-ubiquinone oxidoreductase 51 kDa subunit)	NDUFV1 UQOR1	Up-regulated

Q9NZ01	Very-long-chain enoyl-CoA reductase (EC 1.3.1.93) (Synaptic glycoprotein SC2) (Trans-2,3-enoyl-CoA reductase) (TER)	TECR GPSN2 SC2	Up-regulated
Q9UJU6	Drebrin-like protein (Cervical SH3P7) (Cervical mucin-associated protein) (Drebrin-F) (HPK1-interacting protein of 55 kDa) (HIP-55) (SH3 domain-containing protein 7)	DBNL CMAP SH3P7 PP5423	Up-regulated
P12955	Xaa-Pro dipeptidase (X-Pro dipeptidase) (EC 3.4.13.9) (Imidodipeptidase) (Peptidase D) (Proline dipeptidase) (Prolidase)	PEPD PRD	Up-regulated
P78344	Eukaryotic translation initiation factor 4 gamma 2 (eIF-4-gamma 2) (eIF-4G 2) (eIF4G 2) (Death-associated protein 5) (DAP-5) (p97)	EIF4G2 DAP5 OK/SW-cl.75	Down-regulated
Q16204	Coiled-coil domain-containing protein 6 (Papillary thyroid carcinoma-encoded protein) (Protein H4)	CCDC6 D10S170 TST1	Down-regulated
Q13561	Dynactin subunit 2 (50 kDa dynein-associated polypeptide) (Dynactin complex 50 kDa subunit) (DCTN-50) (p50 dynamitin)	DCTN2 DCTN50	Down-regulated
Q9NPA8	Transcription and mRNA export factor ENY2 (Enhancer of yellow 2 transcription factor homolog)	ENY2 DC6	Down-regulated
P61927	60S ribosomal protein L37 (G1.16) (Large ribosomal subunit protein eL37)	RPL37	Down-regulated
O95373	Importin-7 (Imp7) (Ran-binding protein 7) (RanBP7)	IPO7 RANBP7	Down-regulated
P84090	Enhancer of rudimentary homolog	ERH	Down-regulated
Q6NYC8	Phostensin (Protein phosphatase 1 F-actin cytoskeleton-targeting subunit) (Protein phosphatase 1 regulatory subunit 18)	PPP1R18 HKMT1098 KIAA1949	Down-regulated
Q9UHV9	Prefoldin subunit 2	PFDN2 PFD2 HSPC231	Down-regulated
P53621	Coatomer subunit alpha (Alpha-coat protein) (Alpha-COP) (HEP-COP) (HEPCOP) [Cleaved into: Xenin (Xenopsin-related peptide); Proxenin]	COPA	Down-regulated

Whole list of proteins that were unique in pal_vs_veh when they were compared with the proteins that were expressed differentially of tip_vs_veh with a p_value <0.01 and a FDR <0.1 in both comparisons, suggesting that tibolone pretreatment shifted the expression of these proteins to a level similar to the vehicle.

Supplementary material 5. GO Slim of the regulation of protein transport

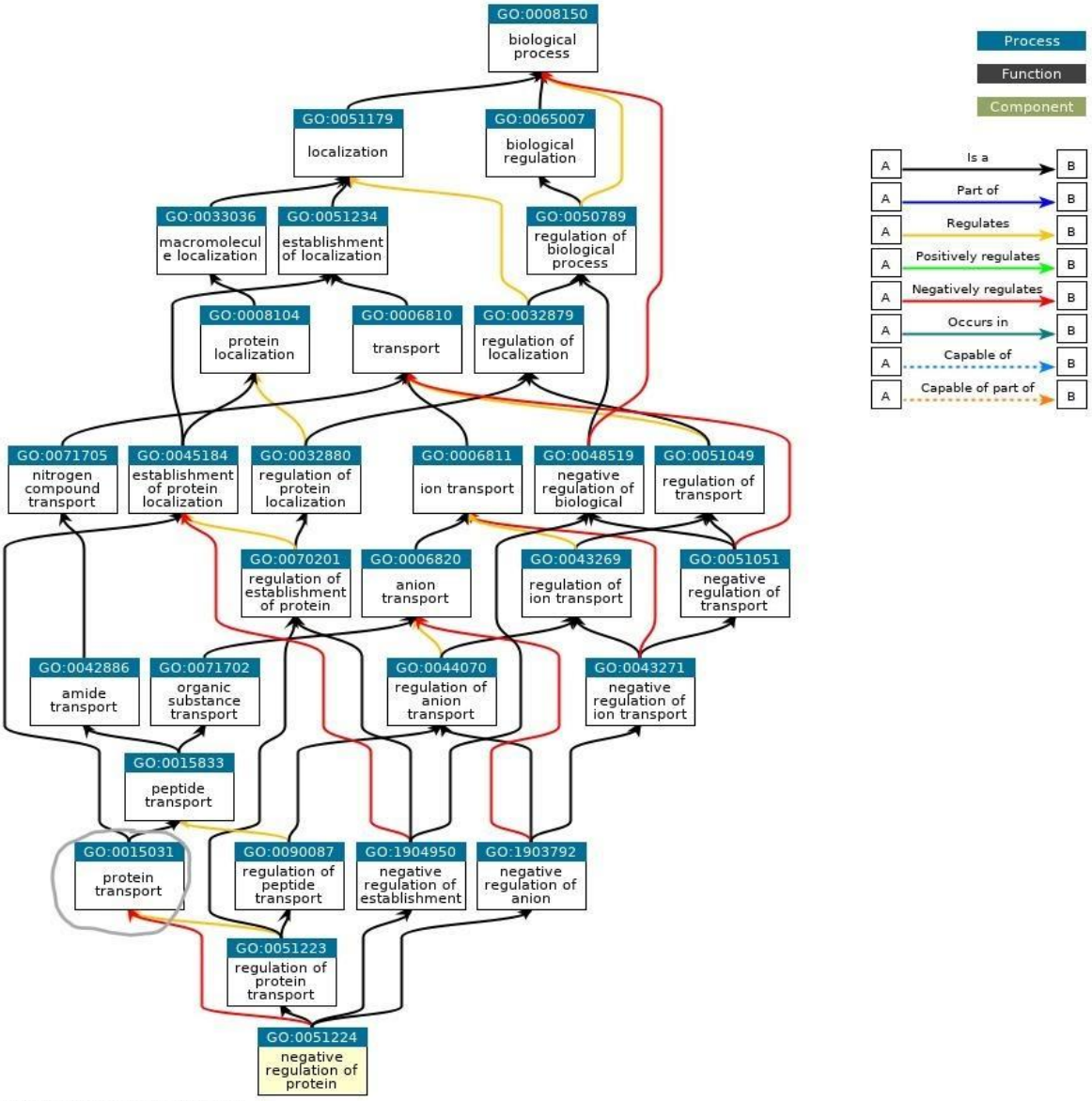

GOSlim related of terms linked to negative regulation of protein and highlighting protein transport to track the terms that can be affected by protein transport changes.

Supplementary material 6.

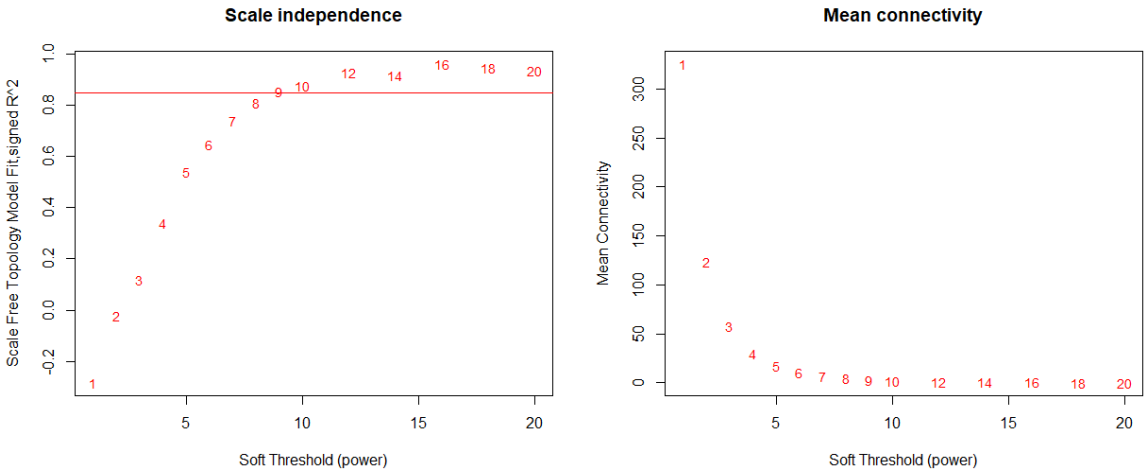

SFT of Scale independence and mean connectivity used for the WGCNA.

Supplementary material 7.

Mcode Cluster	From node	Gene names	Belonging node	Node name	To node
12	O75340	PDCD6 ALG2	turquoise	O75340	O75340
12	P51571	SSR4 TRAPD	turquoise	P51571	P51571
12	P13861	PRKAR2A PKR2 PRKAR2	turquoise	P13861	
11	Q9NY33	DPP3	turquoise	Q9NY33	Q9NY33
11	O43294	TGFB1I1 ARA55	turquoise	O43294	
13		PLCH1 KIAA1069 PLCL3	red	Q4KWH8	Q4KWH8
13	Q9BZK7	TBL1XR1 IRA1 TBLR1	red	Q9BZK7	Q9BZK7
13	P49023	PXN	red	P49023	
4		ALS2 ALS2CR6 KIAA1563	red	Q96Q42	Q96Q42
6	P55263	ADK	red	P55263	P55263
6	O95373	IPO7 RANBP7	red	O95373	O95373
14	P61313	RPL15 EC45 TCBAP0781	red	P61313	P61313
14	P47755	CAPZA2	red	P47755	
4	O60884	DNAJA2 CPR3 HIRIP4	red	O60884	O60884
5		CHCHD3 MIC19 MINOS3	turquoise	Q9NX63	Q9NX63
5	P10253	GAA	turquoise	P10253	P10253
11	Q9NTK5	OLA1 GTPBP9 PRO2455 PTD004	turquoise	Q9NTK5	Q9NTK5
8		EIF3L EIF3EIP EIF3S6IP HSPC021 HSPC025 MSTP005	turquoise	Q9Y262	Q9Y262

8	P84157	MXRA7	turquoise	P84157	P84157
8	P13611	VCAN CSPG2	turquoise	P13611	P13611
8	P09960	LTA4H LTA4	turquoise	P09960	
4	P16035	TIMP2	red	P16035	P16035
6	P61204	ARF3	red	P61204	P61204
14	O43795	MYO1B	red	O43795	O43795
5	Q12792	TWF1 PTK9	turquoise	Q12792	Q12792
5	P21399	ACO1 IREB1	turquoise	P21399	P21399
4	P60484	PTEN MMAC1 TEP1	red	P60484	P60484
6	Q92890	UFD1 UFD1L	red	Q92890	Q92890
6		STUB1 CHIP PP1131	red	Q9UNE7	Q9UNE7
2	P63173	RPL38	pink	P63173	P63173
2	Q9BR76	CORO1B	pink	Q9BR76	Q9BR76
4	O00571	DDX3X DBX DDX3	red	O00571	O00571
2	P08708	RPS17 RPS17L	pink	P08708	P08708
2	P37837	TALDO1 TAL TALDO TALDOR	pink	P37837	P37837
2	P49773	HINT1 HINT PKCI1 PRKCNH1	pink	P49773	P49773
2	P23396	RPS3 OK/SW-cl.26	pink	P23396	P23396
2	P23381	WARS1 IFI53 WARS WRS	pink	P23381	P23381
2	P30086	PEBP1 PBP PEBP	pink	P30086	P30086
2	P07951	TPM2 TMSB	pink	P07951	P07951
2	P26038	MSN	pink	P26038	P26038
2	P13639	EEF2 EF2	pink	P13639	P13639
1		ART4 DO DOK1	turquoise	Q93070	Q93070
1	O95819	MAP4K4 HGK KIAA0687 NIK	turquoise	O95819	O95819
10		PFDN1 PFD1	turquoise	O60925	O60925
1	P49902	NT5C2 NT5B NT5CP PNT5	turquoise	P49902	P49902
1	P18065	IGFBP2 BP2 IBP2	turquoise	P18065	P18065
1	Q7L014	DDX46 KIAA0801	turquoise	Q7L014	Q7L014
7	P36507	MAP2K2 MEK2 MKK2 PRKMK2	pink	P36507	P36507
3	Q9Y646	CPQ LCH1 PGCP	pink	Q9Y646	Q9Y646
1	O95497	VNN1	turquoise	O95497	O95497
7	Q6IBS0	TWF2 PTK9L MSTP011	turquoise	Q6IBS0	Q6IBS0
1	P05413	FABP3 FABP11 MDGI	turquoise	P05413	P05413
1	P62244	RPS15A OK/SW-cl.82	turquoise	P62244	P62244
1	Q9P0K7	RAI14 KIAA1334 NORPEG	turquoise	Q9P0K7	Q9P0K7

1	Q9NVD7	PARVA MXRA2	turquoise	Q9NVD7	Q9NVD7
1	P53985	SLC16A1 MCT1	turquoise	P53985	P53985
1	P32969	RPL9 OK/SW-cl.103; RPL9P7; RPL9P8; RPL9P9	turquoise	P32969	P32969
7	P05121	SERPINE1 PAI1 PLANH1	red	P05121	P05121
1	P30040	ERP29 C12orf8 ERP28	turquoise	P30040	P30040
1	P49327	FASN FAS	turquoise	P49327	P49327
1	O00231	PSMD11	turquoise	O00231	O00231
1	P39687	ANP32A C15orf1 LANP MAPM PHAP1	turquoise	P39687	P39687
1	B5ME19	EIF3CL	turquoise	B5ME19	B5ME19
2	P27635	RPL10 DXS648E QM	turquoise	P27635	P27635
10	Q07666	KHDRBS1 SAM68	turquoise	Q07666	Q07666
2	P49257	LMAN1 ERGIC53 F5F8D	turquoise	P49257	P49257
1	P62195	PSMC5 SUG1	turquoise	P62195	P62195
2	O00159	MYO1C	turquoise	O00159	O00159
1	P12235	SLC25A4 ANT1	turquoise	P12235	P12235
1	P24821	TNC HXB	turquoise	P24821	P24821
1	P11766	ADH5 ADHX FDH	turquoise	P11766	P11766
7	Q04637	EIF4G1 EIF4F EIF4G EIF4GI	turquoise	Q04637	Q04637
1	Q92499	DDX1	turquoise	Q92499	Q92499
10	P15559	NQO1 DIA4 NMOR1	turquoise	P15559	P15559
1	O14974	PPP1R12A MBS MYPT1	turquoise	O14974	O14974
1	P07737	PFN1	turquoise	P07737	P07737
2	Q16527	CSRP2 LMO5 SMLIM	turquoise	Q16527	Q16527
1	Q14247	CTTN EMS1	turquoise	Q14247	Q14247
1	P29692	EEF1D EF1D	turquoise	P29692	P29692
7	Q9Y617	PSAT1 PSA	pink	Q9Y617	Q9Y617
9	Q00341	HDLBP HBP VGL	turquoise	Q00341	Q00341
9	P14136	GFAP	turquoise	P14136	P14136
2	Q99497	PARK7	turquoise	Q99497	Q99497
1	P27348	YWHAQ	turquoise	P27348	P27348
1	P23528	CFL1 CFL	turquoise	P23528	P23528
1	Q06830	PRDX1 PAGA PAGB TDPX2	turquoise	Q06830	Q06830
1	P62258	YWHAE	turquoise	P62258	P62258
3	P50395	GDI2 RABGDIB	turquoise	P50395	P50395
1	P07195	LDHB	turquoise	P07195	P07195

3	P13667	PDIA4 ERP70 ERP72	turquoise	P13667	P13667
1	P55072	VCP	turquoise	P55072	P55072
1	O75083	WDR1	turquoise	O75083	O75083
1	P68104	EEF1A1 EEF1A EF1A LENG7	turquoise	P68104	P68104
9	P63104	YWHAZ	turquoise	P63104	P63104
3	P30101	PDIA3 ERP57 ERP60 GRP58	turquoise	P30101	P30101
2	Q14195	DPYSL3 CRMP4 DRP3 ULIP ULIP1	turquoise	Q14195	Q14195
1	Q13509	TUBB3 TUBB4	turquoise	Q13509	Q13509
1	P07900	HSP90AA1 HSP90A HSPC1 HSPCA	turquoise	P07900	P07900
7	P14625	HSP90B1 GRP94 TRA1	turquoise	P14625	P14625
1	P07437	TUBB TUBB5 OK/SW-cl.56	turquoise	P07437	P07437
1	Q71U36	TUBA1A TUBA3	turquoise	Q71U36	Q71U36
1	P63261	ACTG1 ACTG	turquoise	P63261	
3	P09913	IFIT2 CIG-42 G10P2 IFI54 ISG54	turquoise	P09913	P09913
7	Q9UBI6	GNG12	turquoise	Q9UBI6	Q9UBI6
3	O14879	IFIT3 CIG-49 IFI60 IFIT4 ISG60	turquoise	O14879	O14879
1	P09211	GSTP1 FAEES3 GST3	turquoise	P09211	P09211
1	O14950	MYL12B MRLC2 MYLC2B	turquoise	O14950	O14950
7	P11021	HSPA5 GRP78	turquoise	P11021	P11021
3	P04406	GAPDH GAPD CDABP0047 OK/SW-cl.12	turquoise	P04406	P04406
1	P11142	HSPA8 HSC70 HSP73 HSPA10	turquoise	P11142	P11142

Whole list of nodes that passed the filter imposed by MCODE algorithm in Cytoscape 3.8.0, which represents the hub proteins obtained in this study and that are positively and significantly co-related to changes induced by treatment.